



Magnetite tethered mesoionic carbene-palladium (II): An efficient and reusable nanomagnetic catalyst for Suzuki-Miyaura and Mizoroki-Heck cross-coupling reactions in aqueous medium

Manjunatha Kempasiddhaiah¹ | Vishal Kandathil¹ | Ramesh B. Dateer¹ | Balappa S. Sasidhar² | Shivaputra A. Patil³ | Siddappa A. Patil¹

¹ Centre for Nano and Material Sciences, Jain University, Jain Global Campus, Kanakapura, Ramanagaram, Bangalore 562112, India

² Organic Chemistry Section, Chemical Sciences & Technology Division, National Institute for Interdisciplinary Science and Technology (CSIR), Thiruvananthapuram 695019, Kerala, India

³ Pharmaceutical Sciences Department, College of Pharmacy, Rosalind Franklin University of Medicine and Science, 3333 Green Bay Road, North Chicago, IL 60064, USA

Correspondence

Siddappa A. Patil, Centre for Nano and Material Sciences, Jain University, Jain Global Campus, Kanakapura, Ramanagaram, Bangalore 562112, India. Email: p.siddappa@jainuniversity.ac.in; patilsiddappa@gmail.com

Funding information

Jain University; DST-Nanomission, India, Grant/Award Number: SR/NM/NS-20/2014; DST-SERB, India, Grant/Award Number: YSS/2015/000010

In this paper, a highly active, air- and moisture-stable and easily recoverable magnetic nanoparticles tethered mesoionic carbene palladium (II) complex (MNPs-MIC-Pd) as nanomagnetic catalyst was successfully synthesized by a simplistic multistep synthesis under aerobic conditions using commercially available inexpensive chemicals for the first time. The synthesized MNPs-MIC-Pd nanomagnetic catalyst was in-depth characterized by numerous physicochemical techniques such as FT-IR, ICP-AES, FESEM, EDS, TEM, *p*-XRD, XPS, TGA and BET surface area analysis. The prepared MNPs-MIC-Pd nanomagnetic catalyst was used to catalyze the Suzuki-Miyaura and Mizoroki-Heck cross-coupling reactions and exhibited excellent catalytic activity for various substrates under mild reaction conditions. Moreover, MNPs-MIC-Pd nanomagnetic catalyst could be easily and rapidly recovered by applying an external magnet. The recovered MNPs-MIC-Pd nanomagnetic catalyst exhibited very good catalytic activity up to ten times in Suzuki-Miyaura and five times in Mizoroki-Heck cross-coupling reactions without considerable loss of its catalytic activity. However, MNPs-MIC-Pd nanomagnetic catalyst shows notable advantages such as heterogeneous nature, efficient catalytic activity, mild reaction conditions, easy magnetic work up and recyclability.

KEYWORDS

magnetic nanoparticles, mesoionic carbene-palladium (II), Mizoroki-heck cross-coupling, nanomagnetic catalyst, Suzuki-Miyaura cross-coupling

1 | INTRODUCTION

A catalyst is a chemical substance that can increase the rate of chemical reaction through altering the activation energy which is essential for the chemical reaction to proceed. Unlike the other reagents, catalyst take part in the chemical reaction but is chemically not used up and remains unchanged at the end of the chemical reaction

and could be reused.^[1] In general, catalysts can be broadly classified into two types, homogeneous and heterogeneous depending on the physical state of the catalyst and reactants in the chemical reaction. In homogeneous catalysis, catalyst and all the reactants are in the same phase usually in the liquid phase while in heterogeneous catalysis, catalysts are solid compounds that are mixed with liquid or gas phase reactants.^[2,3] Homogeneous

and heterogeneous catalysts both have advantages and disadvantages. An advantage of homogeneous catalysts is that the catalyst combines well with reaction mixture permitting high degree of association between catalyst and reactants and increases the efficiency of the reaction. However, it is hard to separate homogeneous catalyst from the product and lowers its recovery at the end of the chemical reaction.^[4] On the other hand, the utmost advantage of heterogeneous catalyst is the effortless separation of the catalyst from the reaction mass and the disadvantage being their limited activity and selectivity.^[5] Hence, there is an urgent need for a catalyst which can increase the efficiency of the chemical reaction like homogeneous catalyst and can be isolated easily after reaction completion similar to heterogeneous catalyst.

First free and stable N-heterocyclic carbene (NHC) was isolated by Arduengo and co-workers in 1991 through deprotonation of 1,3-bisadamantyl imidazolium chloride.^[6] After that, N-heterocyclic carbenes (NHCs) have emerged as potent ligand precursors in organometallic chemistry and catalysis. However, since last two decades NHCs have demonstrated significant input over phosphines because of their stability in air- and moisture, less toxicity, higher dissociation energies and strong σ -donor properties which enhances the stability of the resulting metal complexes.^[7-17] In general NHCs can be classified into two categories: classic NHCs and mesoionic carbenes (MICs). NHCs resulting from imidazol-2-ylidenes and 1,2,4-triazol-5-ylidenes belong to the class of classic NHCs. NHCs derived from 1,2,4- and 1,3,4-trisubstituted 1,2,3-triazol-5-ylidenes and imidazol-4-ylidenes belong to the class of MICs.^[18] Recent past, 1,3,4-trisubstituted 1,2,3-triazol-5-ylidenes (MICs) and their corresponding metal complexes have drawn a lot of attention in homogeneous catalysis of various organic reactions such as carbon-carbon (C-C) and carbon-nitrogen (C-N) cross-coupling reactions.^[19] This development may be endorsed from the stronger σ -donor ability of the carbene carbon of 1,3,4-trisubstituted 1,2,3-triazol-5-ylidene than that of classical NHC.^[20-22]

The Suzuki-Miyaura and Mizoroki-Heck cross-coupling reactions are some of the widely used C-C bond forming reactions in organic transformations. These chemical reactions have been applied to the synthesis of complex natural products, engineering materials such as conducting polymers, molecular wires, supramolecular chemistry, liquid crystals and functionalized olefins.^[23-32] Therefore, various types of catalysts have been developed for Suzuki-Miyaura and Mizoroki-Heck cross-coupling reactions. Among these, 1,3,4-trisubstituted 1,2,3-triazol-5-ylidene metal complexes have shown tremendous catalytic activities and various homogeneous catalysts have been developed.^[19,33-36] However, the major

disadvantages of homogeneous catalysts include difficulty of their recovery from the reaction medium for reuse. This problem is of economic and environmental concern in bulk synthesis. To conquer these difficulties, nowadays, magnetic nanoparticles have been used as a catalyst support, which include the advantage of very high surface area and easy recovery and recycling of catalyst. In this way, magnetic separation offers a convenient and efficient method for the recovery of the nanomagnetic catalyst from C-C cross-coupling reaction systems.^[37]

Extensive literature survey reveals that no reports are available on the synthesis and characterization of 1,3,4-trisubstituted 1,2,3-triazol-5-ylidene metal complexes on the surface of magnetic nanoparticles with high catalytic activity in Suzuki-Miyaura and Mizoroki-Heck cross-coupling reactions. Thus in continuation of our investigations on magnetically recyclable nanomagnetic catalysts in various organic transformations, we report here a new magnetic nanoparticle supported 1,3,4-trisubstituted 1,2,3-triazol-5-ylidene-palladium (II) nanomagnetic catalyst whose ligand system is based on mesoionic carbenes which is entirely different from NHCs and Schiff-base ligand system which were reported in our earlier work.^[38-41] The MNPs-MIC-Pd nanomagnetic catalyst was structurally characterized from spectroscopic and microscopic techniques. In addition, The MNPs-MIC-Pd nanomagnetic catalyst exhibited very good catalytic activity in both Suzuki-Miyaura and Mizoroki-Heck cross-coupling reactions. Furthermore, MNPs-MIC-Pd nanomagnetic catalyst can be easily recovered from the reaction mixture by using an external magnet and reused up to ten times in Suzuki-Miyaura and five times in Mizoroki-Heck cross-coupling reactions without much loss in the catalytic activity. The use of environmentally-friendly solvent system Ethanol:water (EtOH:H₂O) (1:1) and recyclable MNPs-MIC-Pd nanomagnetic catalyst at room temperature makes our reaction protocol more interesting for both Suzuki-Miyaura and Mizoroki-Heck cross-coupling reactions. Therefore, our research endeavors have recognized the atom-economy and ideal greener conditions to accomplish an excellent yield for both Suzuki-Miyaura and Mizoroki-Heck cross-coupling reactions. We wish our research results will add great value to the environmentally sustainable and green chemistry research field.

2 | EXPERIMENTAL

2.1 | Materials

Required solvents were purified according to the standard methods prior to use. Unless otherwise stated, all reactions were performed under aerobic or nitrogen atmosphere

conditions in oven-dried glassware with magnetic stirrer. All chemicals were purchased from Sigma-Aldrich and Avra chemical companies and were used without further purification. Heating was accomplished by either a heating mantle or silicone oil bath. Column chromatography was conducted on Silica gel 60–120 mesh (Merck) and preparative thin-layer chromatography was carried out using 0.25 mm Merck TLC silica gel plates using UV light as a visualizing agent. Yields refer to chromatographically pure material. Concentration *in vacuo* refers to the removal of volatile solvent using a rotary evaporator attached to a dry diaphragm pump (10–15 mm Hg) followed by pumping to a constant weight with an oil pump (<300 mTorr). All the organic products were known and identified by comparison of their physical and spectral data with those of authentic samples.

2.2 | Instrumentation and analyses

Fourier-Transform infrared spectra were recorded with PerkinElmer spectrometer. Brunauer–Emmett–Teller surface areas were obtained by physisorption of nitrogen using Microtrac BELSORP MAX instrument. FESEM images along with energy dispersive X-ray spectroscopy to observe morphology and elemental distributions respectively were obtained with JEOL Model-JSM7100F. Transmission electron microscope images were obtained using Jeol/JEM 2100 microscope. X-ray powder diffractometer patterns were obtained using Ultima IV X-Ray Diffractometer. X-ray photoelectron spectroscopy was obtained using PHI 5000 Versa probe- Scanning ESCA MicroProbe. Thermogravimetric analysis was carried out by Thermal analyzer (TGA/DTA) (STA-2500, NETZSCH, Berlin, Germany) with a heating rate of 10.0 °C/min. The palladium content of the MNPs-MIC-Pd nanomagnetic catalyst was determined by Perkin Elmer inductively coupled plasma-atomic emission spectroscopy. ¹H and ¹³C NMR spectra were recorded at 400 MHz, and are reported relative to deuterated chloroform (CDCl₃, δ = 7.27 ppm). ¹H NMR coupling constants (J) are reported in Hertz (Hz) and multiplicities are indicated as follows: s (singlet), d (doublet), t (triplet), m (multiplet).

2.3 | Synthesis of hydroxyl substituted magnetic nanoparticles (MNPs) (1)

Hydroxyl substituted magnetic nanoparticles (MNPs) (1) were synthesized using 2:1 molar ratio of FeCl₃·6H₂O (4.70 g, 17.38 mmol) and FeCl₂·4H₂O (1.73 g, 8.70 mmol) by chemical co-precipitation method. A mixture of FeCl₃·6H₂O and FeCl₂·4H₂O was dispersed in deionized water (80 ml) and the resultant yellow solution was

vigorously stirred for 30 min at 85 °C. Subsequently 25% ammonia solution was added drop wise (up to pH = 10) and stirring was continued for 30 min at 85 °C. Then reaction mixture was cooled to room temperature and obtained black colored MNPs were separated by an external magnet. MNPs were washed thoroughly with distilled water up to neutral pH and further washed with ethanol (2 x 20 ml) and dried over night at 80 °C.

2.4 | Synthesis of 3-(azidopropyl)triethoxysilane (APTES) (3)

3-Chloropropyltriethoxysilane (2) (1.0 g, 4.15 mmol) was taken in two necked round bottom flask (100 ml) and sodium azide (0.40 g, 6.15 mmol) was added. The reaction mixture was refluxed for 48 hr in acetonitrile (CH₃CN) (40 mL) under nitrogen atmosphere in the presence of tetrabutylammonium iodide (0.076 g, 0.20 mmol). Solvent was removed under reduced pressure and crude product obtained was dissolved with diethyl ether (20 ml) followed by hyflo filtration and removal of diethyl ether *in vacuo* to get pure 3-(azidopropyl)triethoxysilane (APTES) (3) as colorless liquid. ¹H NMR (400 MHz, CDCl₃): δ (ppm) = 3.76–3.81 (m, 6H), 3.48–3.51 (t, J = 6 Hz, 2H), 1.81–1.88 (m, 2H), 1.17–1.21 (t, J = 8 Hz, 9H), 0.69–0.73 (t, J = 8 Hz, 2H). ¹³C NMR (100 MHz, CDCl₃): δ (ppm) = 58.57, 53.86, 18.21, 7.95, 7.38.

2.5 | Synthesis of magnetic nanoparticles tagged silyl azide (MNPsSA) (4)

Hydroxyl substituted magnetic nanoparticles (1) (3.0 g) were taken in toluene (60 ml) and sonicated for 1 hr. Then APTES (3) (1.2 g, 4.85 mmol) was added drop wise and resultant reaction mixture was heated at 110 °C for 24 hr under nitrogen atmosphere. The reaction mixture was cooled to room temperature after required time. Obtained brown colored azide functionalized magnetic nanoparticles were collected by using an external magnet, washed with toluene (2 x 20 ml) and acetone (2 x 20 ml) and dried overnight at 45 °C to obtain pure magnetic nanoparticles tagged silyl azide (MNPsSA) (4).

2.6 | Synthesis of magnetic nanoparticles attached 1,2,3-triazole (MNPsT) (6)

Phenyl acetylene (5) (1.5 g, 14.68 mmol) was added to a stirring mixture of MNPsSA (3.0 g) and copper iodide (0.56 g, 2.9 mmol) in dimethylformamide:tetrahydrofuran (DMF:THF) (1:1) (40 ml) solvent mixture at room temperature in the presence of triethylamine (5.94 g,

41.84 mmol). The stirring of reaction mixture was continued for three days at room temperature under nitrogen atmosphere. Obtained brown colored magnetic nanoparticles attached 1,2,3-triazole (MNPsT) was separated by an external magnet and washed with diethyl ether (3 x 20 ml), acetone (2 x 20 ml) and 10% ammonia solution (2 x 20 ml) and dried overnight at 45 °C to get pure magnetic nanoparticles attached 1,2,3-triazole (**6**).

2.7 | Synthesis of magnetic nanoparticles tethered 1,2,3-triazolium salt (MNPsTS) (**7**)

Magnetic nanoparticles attached 1,2,3-triazole (**6**) (3.0 g) was dispersed in CH₃CN (50 ml) and sonicated for 10 min. Then methyl iodide (5.63 g, 39.66 mmol) was added drop wise to the reaction mixture and refluxed for 2 days under nitrogen atmosphere. Obtained solid was separated from the reaction mixture using an external magnet and washed with ether (3 x 20 ml) and dried overnight at 45 °C to get magnetic nanoparticles tethered 1,2,3-triazolium salt (MNPsTS) (**7**).

2.8 | Synthesis of magnetic nanoparticles supported mesoionic carbene-palladium (II) complex (MNPs-MIC-Pd) (**8**)

Palladium (II) acetate (0.616 g, 2.74 mmol) was added to the reaction mixture of magnetic nanoparticles attached 1,2,3-triazolium salt (2.8 g) and sodium carbonate (0.247 g, 2.33 mmol) in acetonitrile (CH₃CN) (50 mL). The reaction mixture was heated at 70 °C for 16 hr. Obtained brown colored solid was separated by an external magnet and washed with CH₃CN (2 x 20 mL) and acetone (2 x 20 ml) and dried over night at 45 °C to obtain pure magnetic nanoparticles supported mesoionic carbene-palladium (II) complex (MNPs-MIC-Pd) (**8**).

2.9 | General procedure for Suzuki–Miyaura cross-coupling reaction

A mixture of aryl halide (1.0 mmol), arylboronic acid (1.1 mmol), MNPs-MIC-Pd nanomagnetic catalyst (0.025 mol% Pd respected to aryl halide) and base (2.2 mmol) was stirred in EtOH:H₂O (1:1) system (10 ml) at room temperature and the reaction progress was monitored by thin layer chromatography. After completion of the reaction, the MNPs-MIC-Pd nanomagnetic catalyst was separated by applying an external magnet followed by addition of dichloromethane (DCM) (2 x 20 ml). The organic layer was washed with water (3 x 10 ml), dried over anhydrous MgSO₄ and the solvent was evaporated under reduced pressure. Then cross-

coupled product was purified by column chromatography to afford the corresponding products in good yields. All the cross-coupled products were known molecules and were confirmed by comparing the melting point and ¹H NMR spectroscopic data with authentic samples.

1. *Biphenyl* (Table 3, entries 1, 2 and 3): Colorless crystals. Melting point = 67–70 °C; ¹H NMR (400 MHz, CDCl₃): δ (ppm) = 7.74–7.72 (m, 4H), 7.55–7.53 (m, 4H), 7.46 (t, *J* = 6.0 Hz, 2H).
2. *4-Methoxybiphenyl* (Table 3, entries 4 and 5): White powder. Melting point = 86–90 °C; ¹H NMR (400 MHz, CDCl₃): δ (ppm) = 7.56–7.52 (m, 4H), 7.43 (t, *J* = 6.0 Hz, 2H), 7.31 (t, *J* = 6.0 Hz, 1H), 6.98 (d, *J* = 4.0 Hz, 2H), 3.84 (s, 3H).
3. *2-Methoxybiphenyl* (Table 3, entry 6): White powder. Melting point = 30–32 °C; ¹H NMR (400 MHz, CDCl₃): δ (ppm) = 7.53 (d, *J* = 4.0 Hz, 2H), 7.42 (t, *J* = 8.0 Hz, 2H), 7.33 (t, *J* = 6.0 Hz, 3H), 7.04 (t, *J* = 6.0 Hz, 1H), 6.99 (d, *J* = 8.0 Hz, 1H), 3.80 (s, 3H).
4. *4-Methylbiphenyl* (Table 3, entry 7 and 8): White crystalline solid. Melting point = 45–47 °C; ¹H NMR (400 MHz, CDCl₃): δ (ppm) = 7.59 (d, *J* = 8.0 Hz, 2H), 7.51(d, *J* = 8.0 Hz, 2H), 7.44 (t, *J* = 6.0 Hz, 3H), 7.34 (t, *J* = 6.0 Hz, 2H), 2.40 (s, 3H).
5. *2-Methylbiphenyl* (Table 3, entry 9): Colorless liquid; ¹H NMR (400 MHz, CDCl₃): δ (ppm) = 7.90 (d, *J* = 8.0 Hz, 2H), 7.70 (d, *J* = 4.0 Hz, 2H), 7.58 (d, *J* = 4.0 Hz, 2H), 7.43 (t, *J* = 6.0 Hz, 2H), 7.37 (t, *J* = 6.0 Hz, 1H), 1.38 (s, 3H).
6. *2-Phenylbenzaldehyde* (Table 3, entry 10): Yellow oil. ¹H NMR (400 MHz, CDCl₃): δ (ppm) = 9.99 (s, 1H), 8.04 (d, *J* = 8.0 Hz, 1H), 7.73 (t, *J* = 4.0 Hz, 2H), 7.66 (t, *J* = 6.0 Hz, 1H), 7.49–7.45 (m, 3H), 7.39 (d, *J* = 4.0 Hz, 2H).
7. *4-Phenylbenzaldehyde* (Table 3, entry 11): Yellow crystals. Melting point = 57–59 °C; ¹H NMR (400 MHz, CDCl₃): δ (ppm) = 10.06 (s, 1H), 7.96 (d, *J* = 4.0 Hz, 2H), 7.77(d, *J* = 8.0 Hz, 2H), 7.65 (d, *J* = 8.0 Hz, 2H), 7.50 (t, *J* = 6.0 Hz, 2H), 7.43(t, *J* = 6.0 Hz, 1H).
8. *4-Acetylbiphenyl* (Table 3, entry 12): White powder. Melting point = 120–123 °C; ¹H NMR (400 MHz, CDCl₃): δ (ppm) = 8.03 (d, *J* = 4.0 Hz, 2H), 7.69 (d, *J* = 8.0 Hz, 2H), 7.63 (d, *J* = 8.0 Hz, 2H), 7.48 (t, *J* = 6.0 Hz, 2H), 7.41 (t, *J* = 6.0 Hz, 1H), 2.63 (s, 3H).
9. *4-Hydroxybiphenyl* (Table 3, entries 13 and 14): White crystals. Melting point = 164–166 °C; ¹H NMR (400 MHz, CDCl₃): δ (ppm) = 7.54 (d, *J* = 4.0 Hz, 2H), 7.48 (d, *J* = 4.0 Hz, 2H), 7.43 (t, *J* = 6.0 Hz, 2H), 7.32 (t, *J* = 6.0 Hz, 1H), 6.91 (d, *J* = 4.0 Hz, 2H), 5.13 (s, 1H).

10. *1-Phenylnaphthalene* (Table 3, entry 15): White solid. Melting point = 42–45 °C; ¹H NMR (400 MHz, CDCl₃): δ (ppm) = 7.91–7.85 (m, 3H), 7.54–7.47 (m, 6H), 7.44 (t, *J* = 4.0 Hz, 3H)
11. *4-Cyanobiphenyl* (Table 3, entry 16): Off-white crystalline powder. Melting point = 85–87 °C; ¹H NMR (400 MHz, CDCl₃): δ (ppm) = 7.74 (d, *J* = 8.0 Hz, 2H), 7.69 (d, *J* = 4.0 Hz, 2H), 7.60 (d, *J* = 8.0 Hz, 2H), 7.50 (t, *J* = 6.0 Hz 2H), 7.44 (t, *J* = 6.0 Hz 1H).
12. *4-(tert-butyl)-1,1'-biphenyl* (Table 3, entry 17): Light brown powder, Melting point = 50–52 °C; ¹H NMR (400 MHz, CDCl₃): δ (ppm) = 7.60 (d, *J* = 8.0 Hz, 2H), 7.55 (d, *J* = 8.0 Hz, 2H), 7.48 (d, *J* = 8.0 Hz, 2H), 7.44 (t, *J* = 6.0 Hz, 2H), 7.34 (t, *J* = 6.0 Hz, 1H), 1.37 (s, 9H).
13. *2,4-Difluoro-1,1'-biphenyl* (Table 3, entry 18): Pale yellow crystals. Melting point = 61–63 °C; ¹H NMR (400 MHz, CDCl₃): δ (ppm) = 7.47 (d, *J* = 4.0 Hz, 2H), 7.41 (d, *J* = 4.0 Hz, 2H), 7.36 (t, *J* = 6.0 Hz, 2H), 7.25 (t, *J* = 6.0 Hz, 2H), 6.84 (d, *J* = 4.0 Hz, 1H).
14. *4-Nitrobiphenyl* (Table 3, entry 19): Pale yellow crystals. Melting point = 110–113 °C; ¹H NMR (400 MHz, CDCl₃): δ (ppm) = 8.30 (d, *J* = 8.0 Hz, 2H), 7.74 (d, *J* = 8.0 Hz, 2H), 7.63 (d, *J* = 8.0 Hz, 2H), 7.51 (t, *J* = 6.0 Hz, 2H), 7.46 (t, *J* = 6.0 Hz, 1H).
15. *4-Chloro-1,1'-biphenyl* (Table 3, entries 20): Colorless crystals. Melting point = 76–78 °C; ¹H NMR (400 MHz, CDCl₃): δ (ppm) = 7.55–7.50 (m, 4H), 7.45–7.33 (m, 5H)
16. *4-Chloro-4'-methoxy-1,1'-biphenyl* (Table 3, entry 21): White solid. Melting point = 91–93 °C; ¹H NMR (400 MHz, CDCl₃): δ (ppm) = 7.49–7.45 (m, 4H), 7.38 (d, *J* = 8.0 Hz, 2H), 6.98 (d, *J* = 8.0 Hz, 2H), 3.84 (s, 3H).
17. *17.4'-Chloro-[1,1'-biphenyl]-4-carbonitrile* (Table 3, entry 22): White solid. Melting point = 133–135 °C; ¹H NMR (400 MHz, CDCl₃): δ (ppm) = 7.73 (d, *J* = 8.0 Hz, 2H), 7.65 (d, *J* = 8.0 Hz, 2H), 7.52 (d, *J* = 8.0 Hz, 2H), 7.45 (d, *J* = 8.0 Hz, 2H).
18. *[1,1'-Biphenyl]-4-carboxylic acid* (Table 3, entry 23): White solid. Melting point = 220–225 °C; ¹H NMR (400 MHz, CDCl₃): δ (ppm) = 12.39 (s, 1H), 7.76–7.74 (m, 4H), 6.79–6.75 (m, 5H).
19. *4'-Methoxy-[1,1'-biphenyl]-4-carboxylic acid* (Table 3, entry 24): White solid. Melting point = 251–254 °C; ¹H NMR (400 MHz, CDCl₃): δ (ppm) = 12.57 (s, 1H), 7.96 (d, *J* = 8.0 Hz, 2H), 7.67 (d, *J* = 8.0 Hz, 2H), 7.03 (d, *J* = 8.0 Hz, 2H), 6.79 (d, *J* = 8.0 Hz, 2H), 3.78 (s, 3H).
20. *4'-Cyano-[1,1'-biphenyl]-4-carboxylic acid* (Table 3, entry 25): Colorless crystals. Melting point = 261–263 °C; ¹H NMR (400 MHz, CDCl₃): δ (ppm) = 12.43 (s, 1H), 7.76 (m, 4H), 6.79 (m, 4H).

2.10 | General procedure for Mizoroki-Heck cross-coupling reaction

Aryl halide (1.0 mmol), alkene (1.2 mmol), MNPs-MIC-Pd nanomagnetic catalyst (0.05 mol% of Pd respected to aryl halide) and base (2.0 mmol) were taken in EtOH:H₂O (1:1) (10 ml). Then reaction mixture was stirred at room temperature for required time and progress of reaction was monitored by thin layer chromatography. After reaction, MNPs-MIC-Pd nanomagnetic catalyst was separated by an external magnet. The reaction mixture was diluted with water and the resultant mixture was extracted with dichloromethane (20 ml) to isolate the product, dried over anhydrous MgSO₄, filtered off and evaporated under reduced pressure. The crude products were purified by column chromatography to afford the corresponding products in good yields. All the cross-coupled products were known molecules and were confirmed by comparing the melting points and ¹H NMR spectroscopic data with authentic samples.

1. *(E)-1,2-diphenylethene* (Table 6, entries 1, 2 and 3): White solid; ¹H NMR (400 MHz, CDCl₃): δ (ppm) = 7.53 (d, *J* = 8.0 Hz, 4H), 7.38 (t, *J* = 6.0 Hz, 4H), 7.28 (t, *J* = 6.0 Hz, 2H), 7.12 (s, 2H).
2. *(E)-1-methyl-4-styrylbenzene* (Table 6, entries 4 and 5): White solid; ¹H NMR (400 MHz, CDCl₃): δ (ppm) = 7.51 (d, *J* = 4.0 Hz, 2H), 7.42 (d, *J* = 4.0 Hz, 2H), 7.37 (t, *J* = 6.0 Hz, 2H), 7.24 (t, *J* = 4.0 Hz, 1H), 7.18 (d, *J* = 8.0 Hz, 2H), 7.08 (d, *J* = 4.0 Hz, 2H), 2.36 (s, 3H).
3. *(E)-1-methoxy-4-styrylbenzene* (Table 6, entries 6 and 7): White crystalline solid; ¹H NMR (400 MHz, CDCl₃): δ (ppm) = 7.50–7.45 (m, 4H), 7.36 (t, *J* = 6.0 Hz, 2H), 7.25 (t, *J* = 6.0 Hz, 1H), 7.06 (d, *J* = 28 Hz, 2H), 6.91 (d, *J* = 8.0 Hz, 2H), 3.83 (s, 3H).
4. *(E)-4-styrylbenzonitrile* (Table 6, entry 9): Yellow solid; ¹H NMR (400 MHz, CDCl₃): δ (ppm) = 7.74–7.72 (m, 2H), 7.61 (d, *J* = 8.0 Hz, 1H), 7.55–7.52 (m, 2H), 7.30 (d, *J* = 4.0 Hz, 2H), 7.08–7.06 (m, 2H), 6.61 (d, *J* = 8.0 Hz, 2H).
5. *Tert-butyl cinnamate* (Table 6, entries 11, 12 and 13): Off-white solid; ¹H NMR (400 MHz, CDCl₃): δ (ppm) = 7.53 (d, *J* = 12 Hz, 1H), 7.45–7.43 (m, 2H), 7.31–7.29 (m, 3H), 6.32 (d, *J* = 12 Hz, 1H), 1.35 (s, 9H).
6. *(E)-tert-butyl 3-(p-tolyl)acrylate* (Table 6, entries 14 and 15): Light yellow liquid; ¹H NMR (400 MHz, CDCl₃): δ (ppm) = 7.58 (d, *J* = 16 Hz, 1H), 7.41 (d, *J* = 4.0 Hz, 2H), 7.18 (d, *J* = 4.0 Hz, 2H), 6.34 (d, *J* = 12 Hz, 1H), 2.37(s, 3H), 1.53 (s, 9H).
7. *(E)-tert-butyl 3-(4-cyanophenyl)acrylate* (Table 6, entry 16): Colorless crystals; ¹H NMR (400 MHz, CDCl₃): δ (ppm) = 7.74–7.72 (m, 1H), 7.61 (d, *J* = 8.0 Hz, 1H),

7.55–7.52 (m, 2H), 7.30 (d, $J = 4.0$ Hz, 1H), 6.61 (d, $J = 4.0$ Hz, 1H), 1.42 (s, 9H).

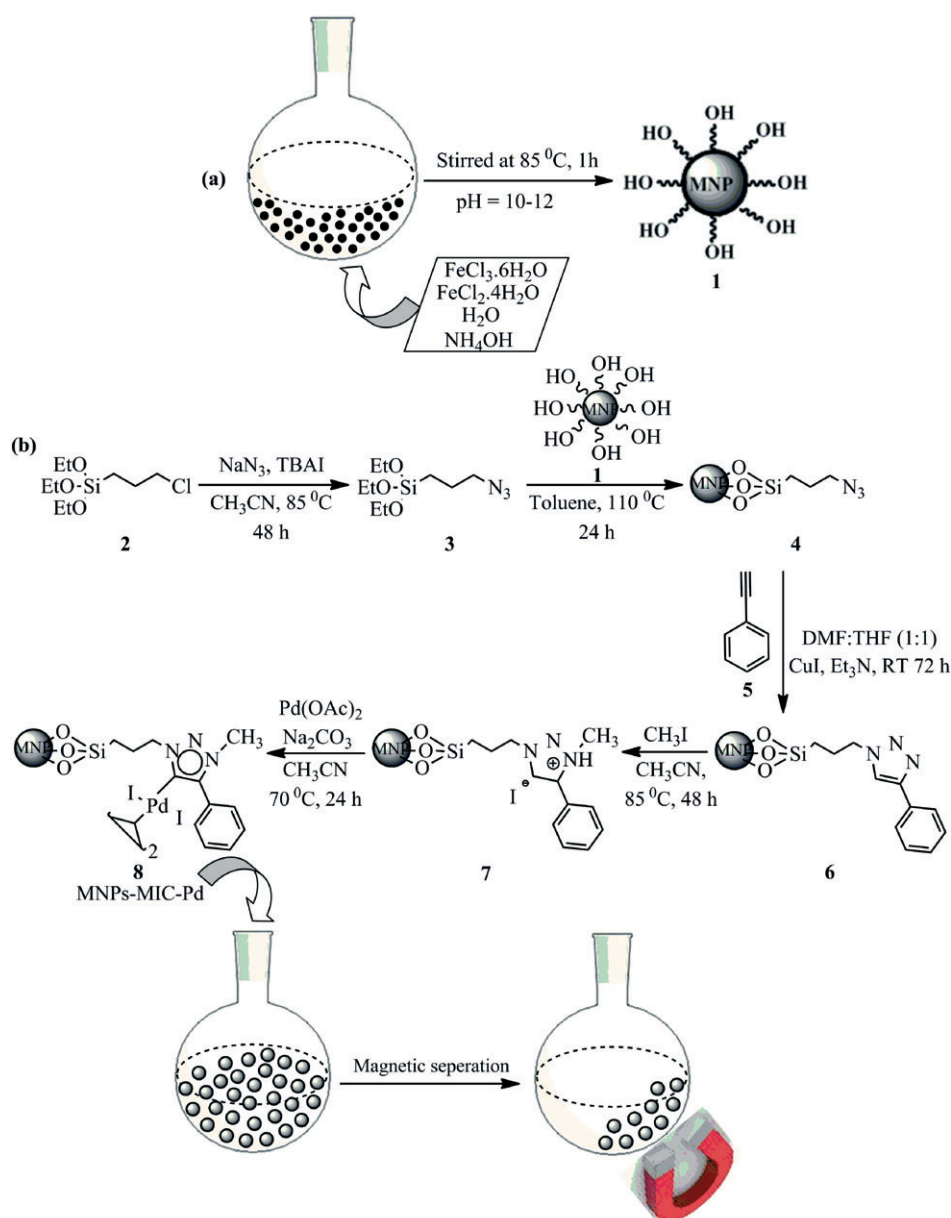
2.11 | Recovery of the MNPs-MIC-Pd nanomagnetic catalyst

After the completion of reaction, MNPs-MIC-Pd nanomagnetic catalyst was separated from reaction mixture using an external magnet. The MNPs-MIC-Pd nanomagnetic catalyst was then washed thoroughly with water (2 x 10 ml), followed by ethanol (2 x 10 ml). The separated MNPs-MIC-Pd nanomagnetic catalyst was dried over night at 45 °C. The dried MNPs-MIC-Pd nanomagnetic catalyst could be used for next round of reaction without further purification.

3 | RESULTS AND DISCUSSION

3.1 | Synthesis of MNPs-MIC-Pd nanomagnetic catalyst

Continuing our work on functionalizing magnetic nanoparticles with variety of derivatives for catalytic applications,^[38–42] in the research accounted here we determined to demonstrate the synthesis of magnetic nanoparticles by attaching mesoionic carbene-palladium (II) complex on the surface of hydroxyl substituted magnetic nanoparticles for the first time. The MNPs-MIC-Pd nanomagnetic catalyst was prepared following the procedure shown in Scheme 1. Firstly, hydroxyl substituted magnetic nanoparticles (**1**) were synthesized by using



SCHEME 1 Synthetic route of a) MNPs (**1**) and b) MNPs-MIC-Pd nanomagnetic catalyst (**8**)

2:1 molar ratio of $\text{FeCl}_3 \cdot 6\text{H}_2\text{O}$ and $\text{FeCl}_2 \cdot 4\text{H}_2\text{O}$ in the presence of ammonia solution by chemical co-precipitation method. On the other hand, (3-azidopropyl)triethoxysilane (**3**) was synthesized using (3-chloropropyl)triethoxysilane (**2**) and sodium azide in acetonitrile at 85 °C for 48 hr. The magnetic nanoparticles tagged silyl azide (**4**) was synthesized by the reaction of hydroxyl substituted magnetic nanoparticles (**1**) with (3-azidopropyl)triethoxysilane (**3**) in toluene at 110 °C for 24 hr. Then “click” reaction was employed between magnetic nanoparticles tagged silyl azide (**4**) and phenyl acetylene (**5**) using copper(I) iodide and triethylamine in a DMF:THF (1:1) solvent mixture at room temperature for 72 hr to get magnetic nanoparticles attached 1,2,3-triazole (**6**). Subsequently, magnetic nanoparticles tethered 1,2,3-triazolium salt (**7**) was prepared through the reaction of magnetic nanoparticles attached 1,2,3-triazole (**6**) with methyl iodide in acetonitrile at 85 °C for 48 hr. Lastly, magnetic nanoparticles tethered 1,2,3-triazolium salt (**7**) was treated with palladium (II) acetate in acetonitrile at 70 °C for 24 hr in the presence of sodium carbonate to get the desired MNPs-MIC-Pd nanomagnetic catalyst (**8**).

3.2 | Spectroscopic and microscopic characterization of the MNPs-MIC-Pd nanomagnetic catalyst

3.2.1 | FT-IR spectroscopy

The chemical structures of products formed in each step were characterized using FT-IR spectroscopic technique. Figure 1 shows FT-IR spectra of MNPs, APTES, MNPsSA, MNPsT, MNPsTS and MNPs-MIC-Pd nanomagnetic catalyst. Figure 1a demonstrates two characteristic peaks

around 598 cm^{-1} and 3400 cm^{-1} which are attributed to the Fe-O and O-H stretching vibrations of hydroxyl substituted magnetic nanoparticles. A medium sharp peak observed at 2097 cm^{-1} corresponds to the azide group of (3-azidopropyl)triethoxysilane (Figure 1b). The characteristic peaks of Fe-O, O-H, Si-O and N_3 stretching vibrations observed at 583 cm^{-1} , 3413 cm^{-1} , 1005 cm^{-1} and 2097 cm^{-1} respectively confirms the successful formation of magnetic nanoparticles tagged silyl azide (Figure 1c). Typical bands observed at 1632 cm^{-1} and 1704 cm^{-1} corresponds to the aromatic ring stretching of magnetic nanoparticles attached 1,2,3-triazole (Figure 1d). FT-IR spectrum of magnetic nanoparticles tethered 1,2,3-triazolium salt (Figure 1e) reveals the slight

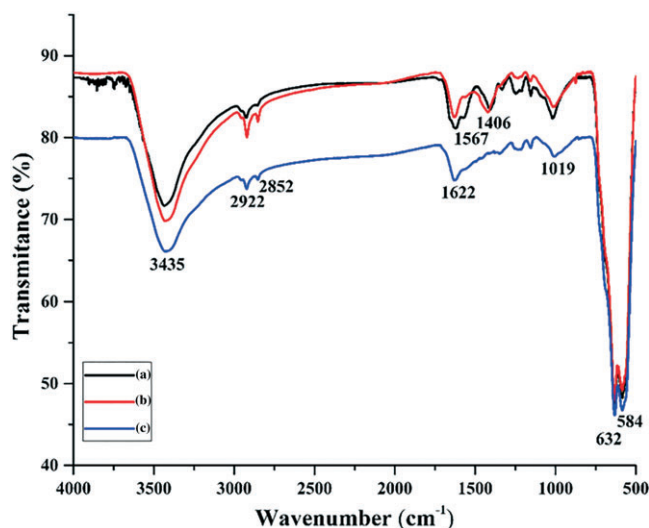


FIGURE 2 FT-IR spectra of a) MNPs-MIC-Pd nanomagnetic catalyst, b) Suzuki-Miyaura recycled MNPs-MIC-Pd nanomagnetic catalyst and c) Mizoroki-Heck recycled MNPs-MIC-Pd nanomagnetic catalyst

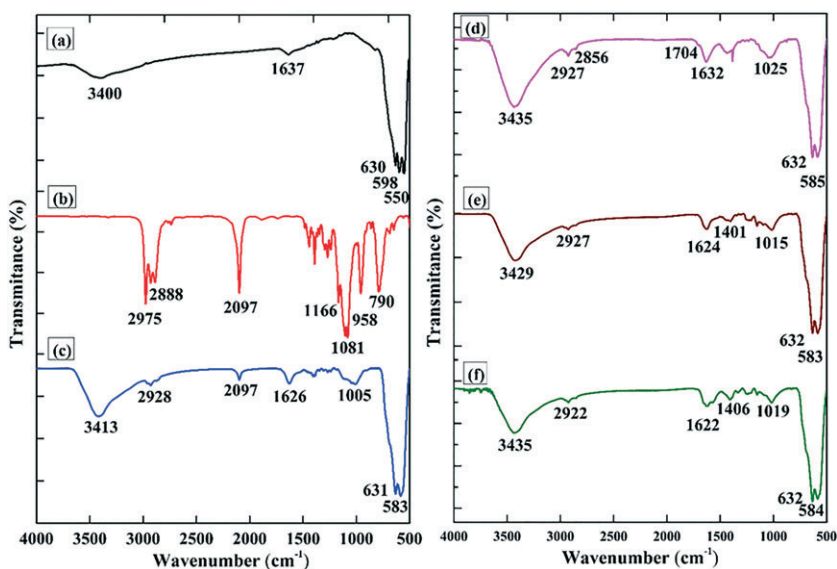


FIGURE 1 FT-IR spectra of a) MNPs, b) APTES, c) MNPsSA, d) MNPsT, e) MNPsTS and f) MNPs-MIC-Pd nanomagnetic catalyst

shifting of aromatic ring stretching from 1632 cm^{-1} to the lower wave number 1624 cm^{-1} ; this confirms the structure of magnetic nanoparticles tethered 1,2,3-triazolium salt. FT-IR spectrum of MNPs-MIC-Pd nanomagnetic catalyst displays the presence of O-H and aliphatic C-H stretching at 3435 cm^{-1} and 2922 cm^{-1} respectively. In addition, existence of typical bands at 1622 cm^{-1} , 1406 cm^{-1} , 1019 cm^{-1} and 584 cm^{-1} are attributed to aromatic ring stretching, Pd-C stretching, Si-O stretching and Fe-O stretching vibrations (Figure 1f) respectively which confirms the successful formation of MNPs-MIC-Pd nanomagnetic catalyst. Figure 2 shows the FT-IR spectra of MNPs-MIC-Pd nanomagnetic catalyst and recycled MNPs-MIC-Pd nanomagnetic catalyst. FT-IR spectra of ten times recycled MNPs-MIC-Pd nanomagnetic catalyst from Suzuki-Miyaura cross-coupling (Figure 2b) and five times recycled MNPs-MIC-Pd nanomagnetic catalyst from Mizoroki-Heck cross-coupling reactions (Figure 2c) confirmed that MNPs-MIC-Pd nanomagnetic catalyst was unaltered and remained almost same even after ten cycles in Suzuki-Miyaura and five cycles in Mizoroki-Heck cross-coupling reactions.^[38,40,43]

3.2.2 | Thermogravimetric analysis

Thermal stability of MNPs and MNPs-MIC-Pd nanomagnetic catalyst was determined by thermogravimetric analysis (TGA) under N_2 atmosphere at the heating rate of $10\text{ }^\circ\text{C}/\text{minute}$ from the range of $35\text{ }^\circ\text{C}$ to $730\text{ }^\circ\text{C}$. TGA graph of MNPs (Figure 3a) shows the weight loss of 3% due to removal of hydroxyl groups present on the surface of MNPs. TGA curve of MNPs-MIC-Pd nanomagnetic catalyst (Figure 3b) shows the decomposition of nanomagnetic catalyst in two stages. Initially 2% weight

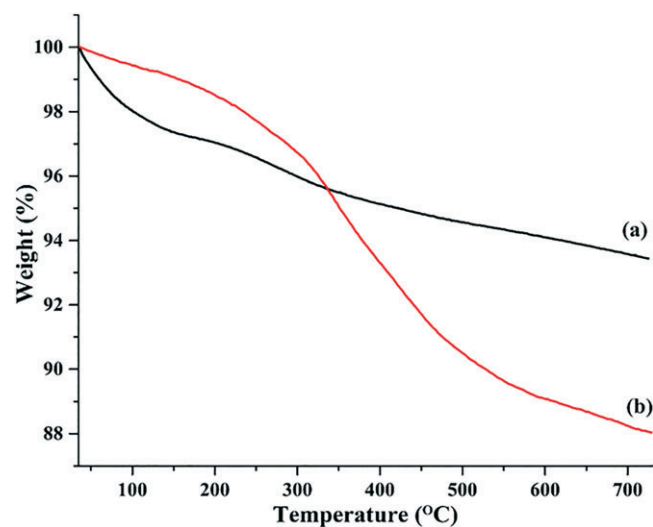


FIGURE 3 TGA curves of a) MNPs and b) MNPs-MIC-Pd nanomagnetic catalyst

loss can be observed in the range $35\text{ }^\circ\text{C}$ to $150\text{ }^\circ\text{C}$ that is due to presence of physically absorbed solvent molecules as well as hydroxyl groups present on the surface of MNPs. In the second stage, up to 11% weight loss of the MNPs-MIC-Pd nanomagnetic catalyst can be observed from the range of $150\text{ }^\circ\text{C}$ to $730\text{ }^\circ\text{C}$ and this is because of the decomposition of organic moiety immobilized on surface of MNPs. Moreover, TGA result confirms the successful immobilization of organic moiety on the surface of MNPs and also reveals that MNPs-MIC-Pd nanomagnetic catalyst is stable up to $230\text{ }^\circ\text{C}$ which helps to carry out the cross-coupling reactions even at higher temperature.^[38,40]

3.2.3 | TEM analysis

The morphology and size of MNPs and MNPs-MIC-Pd nanomagnetic catalyst were investigated by transmission electron microscopy (TEM) (Figure 4). The size of the hydroxyl substituted magnetic nanoparticles varies from 7–10 nm and they are spherical in nature (Figure 4a). After anchoring of the MIC-Pd (II) complex, the size of the nanoparticles was increased from 10–18 nm with quasi spherical in nature (Figure 4b). In addition, the magnetic core as a dark spot inside the spherical MNPs-MIC-Pd nanomagnetic catalyst can be seen from the TEM image. Moreover, MNPs-MIC-Pd nanomagnetic catalyst is polycrystalline in nature which is confirmed by the selected area electron diffraction pattern shown in Figure 4c.^[38–40,43]

3.2.4 | FESEM analysis

FESEM analysis was carried out to get more information regarding surface morphologies of fresh MNPs-MIC-Pd nanomagnetic catalyst and recycled MNPs-MIC-Pd nanomagnetic catalyst (Figure 5.) The FESEM image of fresh MNPs-MIC-Pd nanomagnetic catalyst (Figure 5a) exhibits the formation of uniform nanometer sized spherical particles. Surprisingly, ten times recycled MNPs-MIC-Pd nanomagnetic catalyst (Figure 5b) from Suzuki-Miyaura cross-coupling reaction and five times recycled MNPs-MIC-Pd nanomagnetic catalyst (Figure 5c) from Mizoroki-Heck cross-coupling reaction demonstrates the same morphology and size.^[38–41]

3.2.5 | Elemental analysis

Energy-dispersive X-ray spectroscopy (EDS) was employed to confirm the existence of each element present in the newly synthesized MNPs-MIC-Pd nanomagnetic catalyst. The EDS spectrum (Figure 6) of the MNPs-MIC-Pd nanomagnetic catalyst exhibits characteristic signals

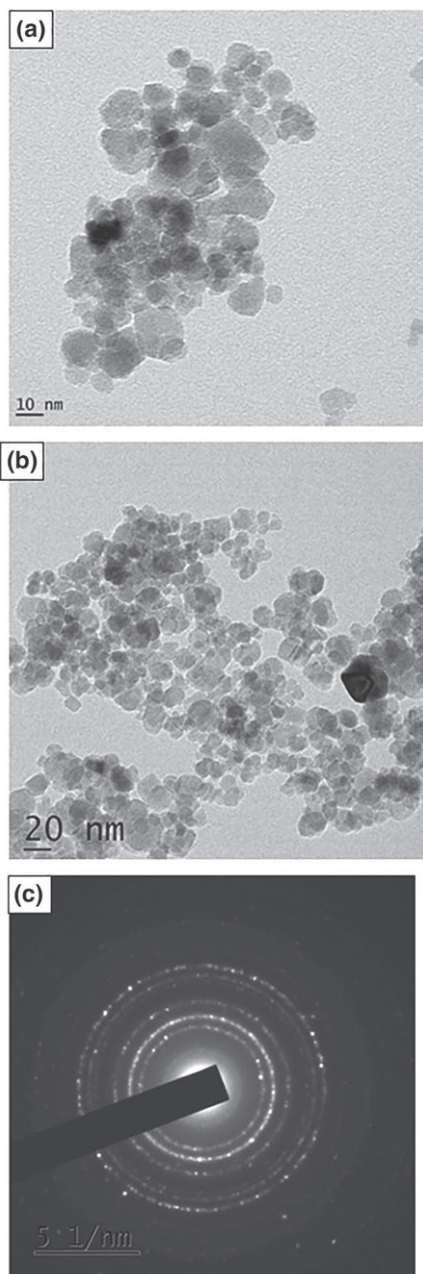


FIGURE 4 TEM images of a) MNPs, b) MNPs-MIC-Pd nanomagnetic catalyst and c) SAED pattern of MNPs-MIC-Pd nanomagnetic catalyst

corresponding to C, N, O, Si, Fe and Pd atoms which proves the attachment of MIC-Pd (II) complex on the surface of the MNPs.^[44] Furthermore, elemental mapping was done to understand the distribution of elements present in the MNPs-MIC-Pd nanomagnetic catalyst as shown in Figure 7. The elemental mapping result demonstrates that all elements are distributed uniformly.^[40]

3.2.6 | BET surface area analysis

The surface functionalization of MNPs, MNPsSA and MNPs-MIC-Pd nanomagnetic catalyst was investigated

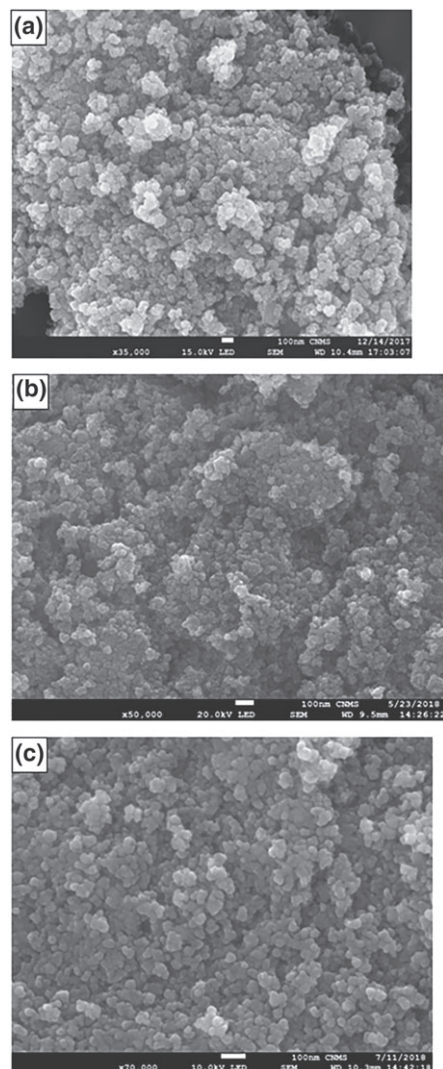


FIGURE 5 FESEM images of a) MNPs-MIC-Pd nanomagnetic catalyst, b) ten times recycled MNPs-MIC-Pd nanomagnetic catalyst from Suzuki-Miyaura and c) five times recycled MNPs-MIC-Pd nanomagnetic catalyst from Mizoroki-Heck cross-coupling reactions

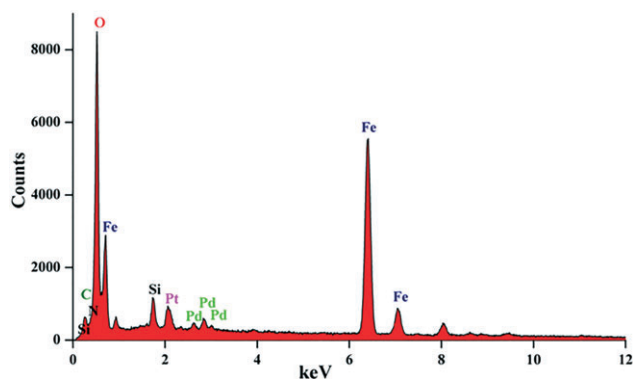


FIGURE 6 EDS spectrum of the MNPs-MIC-Pd nanomagnetic catalyst

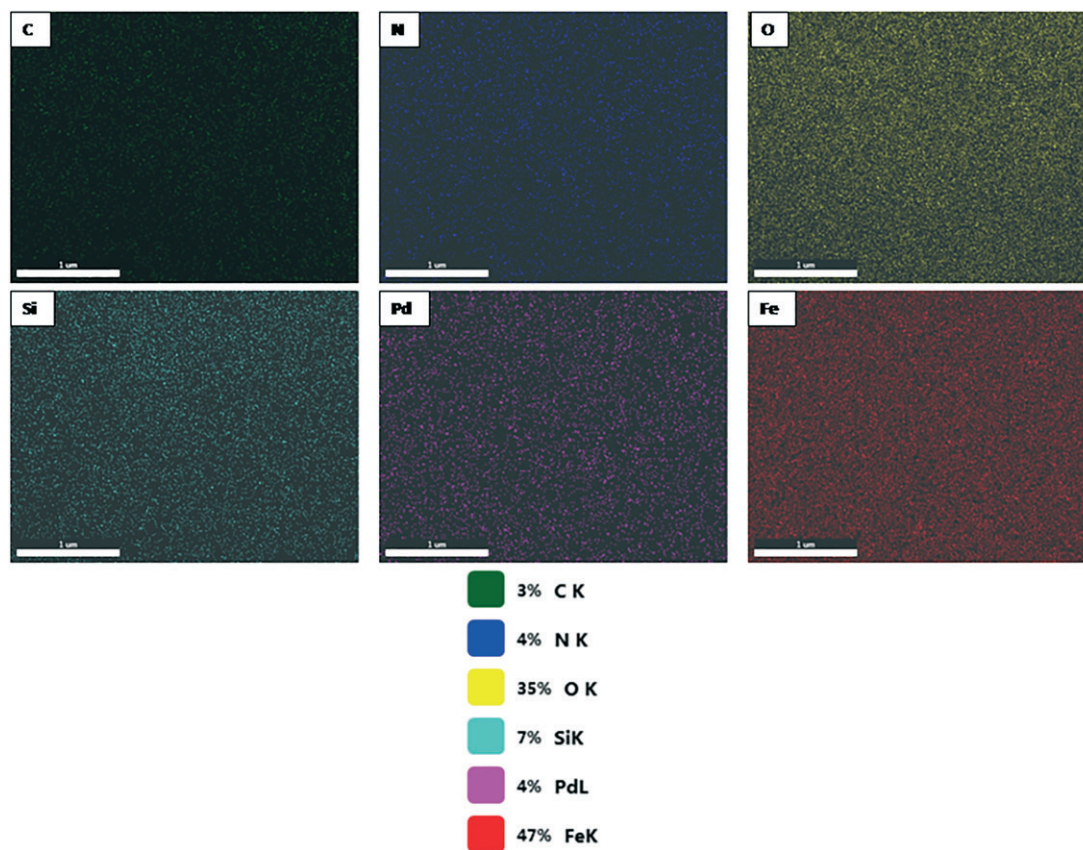


FIGURE 7 EDS elemental mapping of the MNPs-MIC-Pd nanomagnetic catalyst

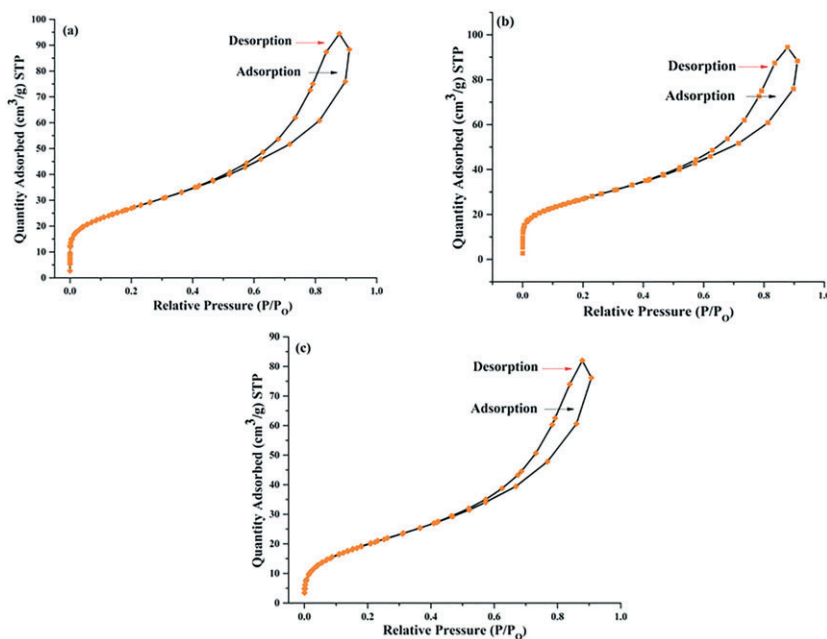


FIGURE 8 Nitrogen adsorption-desorption curves for a) MNPs, b) MNPsSA and c) MNPs-MIC-Pd nanomagnetic catalyst

through Brunauer–Emmett–Teller surface area analysis (BET). Figure 8a–8c demonstrate the nitrogen adsorption-desorption curves for MNPs, MNPsSA and MNPs-MIC-Pd nanomagnetic catalyst respectively. BET result articulates that the amount of N_2 adsorbed on

MNPs-MIC-Pd nanomagnetic catalyst is greater than amount of N_2 adsorbed on MNPs. BET graph for MNPs-MIC-Pd nanomagnetic catalyst exhibit the presence of type-II isotherm. Moreover, the surface area of MNPs decreased from $94.51 \text{ m}^2 \text{ g}^{-1}$ to $93.13 \text{ m}^2 \text{ g}^{-1}$ through

surface functionalization of silyl azide which got further decreased to $74.42 \text{ m}^2 \text{ g}^{-1}$ after functionalization of MIC-Pd (II) complex on the surface of MNPs and thus confirms the formation of MNPs-MIC-Pd nanomagnetic catalyst.^[40]

3.2.7 | ICP-AES analysis

The exact quantity of palladium loaded on the MNPs-MIC-Pd nanomagnetic catalyst was determined through inductively coupled plasma-atomic emission spectroscopy analysis (ICP-AES). This analysis demonstrates a loading of 4.87% (w/w) palladium on the MNPs-MIC-Pd nanomagnetic catalyst.

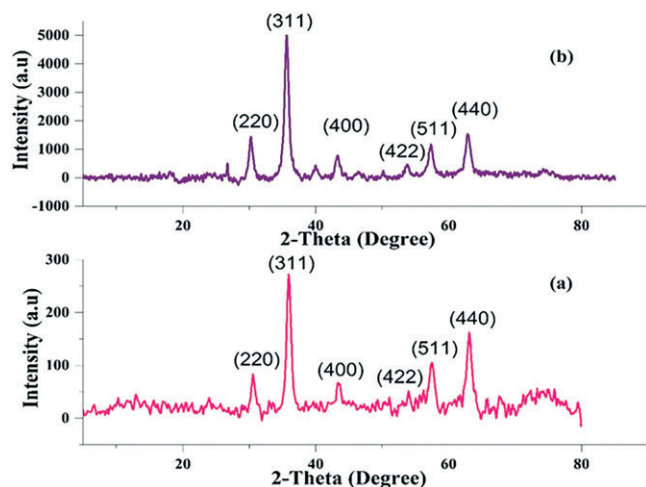


FIGURE 9 XRD patterns of a) MNPs and b) MNPs-MIC-Pd nanomagnetic catalyst

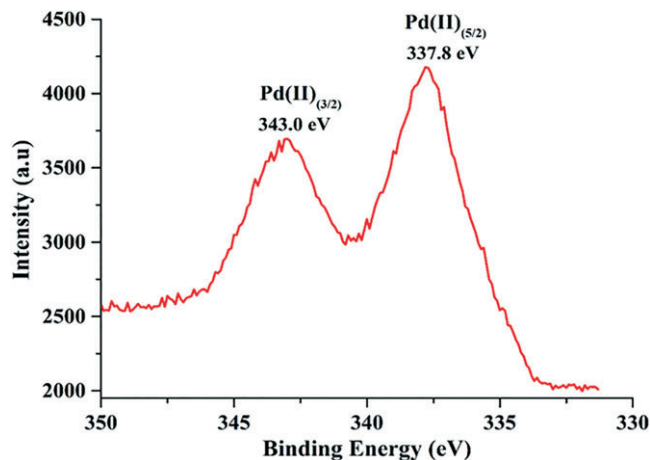
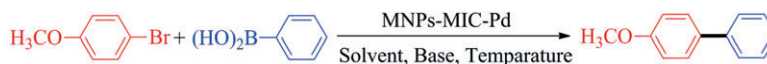


FIGURE 10 XPS spectra for Pd(3d) core level in MNPs-MIC-Pd nanomagnetic catalyst

SCHEME 2 Suzuki-Miyaura cross-coupling reaction of 4-bromoanisole with phenylboronic acid



3.2.8 | XRD analysis

X-ray powder diffraction (XRD) technique was used to determine the crystalline structure of both MNPs and MNPs-MIC-Pd nanomagnetic catalyst. The X-ray powder diffraction pattern for MNPs and MNPs-MIC-Pd nanomagnetic catalyst are shown in Figure 9a and 9b respectively. XRD pattern for MNPs illustrates the different peaks at 2θ of 30.09° , 35.59° , 43.07° , 53.43° , 57.37° and 62.90° corresponding to the different crystal planes (220), (311), (400), (422), (511) and (440) respectively. Moreover, the XRD result confirms the MNPs are exists in cubic spinel structure. The XRD pattern of MNPs-MIC-Pd nanomagnetic catalyst reveals that there is no much difference in crystal structure of MNPs-MIC-Pd nanomagnetic catalyst as compared with crystal structure of MNPs.^[38–40]

3.2.9 | XPS analysis

X-ray photoelectron spectroscopy was carried out to identify the oxidation state of palladium species present in MNPs-MIC-Pd nanomagnetic catalyst and the obtained XPS spectra for Pd on MNPs-MIC-Pd nanomagnetic catalyst is shown in Figure 10. The palladium XPS spectra only show the peaks of Pd (II) corresponding to the binding energy of 343.0 eV (Pd 3d_{3/2}) and 337.8 eV (Pd 3d_{5/2}) suggesting the existence of palladium (II) and confirming there is no any metallic palladium(0) present in the nanomagnetic catalyst which may be formed during the preparation of the MNPs-MIC-Pd nanomagnetic catalyst.^[45,46]

3.3 | Application of the MNPs-MIC-Pd nanomagnetic catalyst in Suzuki–Miyaura cross-coupling reactions

In continuation of our studies on the application of transition metal complexes immobilized on MNPs in organic transformations, herein we report a simple and efficient method for the Suzuki–Miyaura cross-coupling reactions through coupling of aryl halides with arylboronic acids in the presence of catalytic amounts of MNPs-MIC-Pd nanomagnetic catalyst. Thus, catalytic activity of newly synthesized MNP-MIC-Pd nanomagnetic catalyst was established in Suzuki–Miyaura cross-coupling reactions using environmentally friendly reaction conditions. The

reaction conditions were optimized through model Suzuki–Miyaura cross-coupling reaction of 4-bromoanisole with phenylboronic acid as shown in Scheme 2.

Currently, across the world many researchers have shown interest to use green solvents for many organic transformations to avoid hazardous and toxic solvents because of environmental concern. Therefore, during the optimization of reaction conditions, environmentally benign solvents were given highest priority. Consequently, EtOH and H₂O were given highest priority as a green solvent system. The reaction conditions were

optimized with a series of Suzuki–Miyaura cross-coupling reactions of 4-bromoanisole with phenylboronic acid in the presence of MNPs–MIC–Pd nanomagnetic as shown in Table 1. The preliminary results revealed that using Na₂CO₃ base and EtOH:H₂O (1:1) solvent mixture, 0.025 mol% Pd of MNPs–MIC–Pd nanomagnetic catalyst at room temperature for 10 min resulted in highest yield (Table 1, entry 3). The catalytic activity of the MNPs–MIC–Pd nanomagnetic catalyst with varying base, solvent, temperature, time and catalyst ratio was also studied for the model reaction.

TABLE 1 Optimization of conditions for the model Suzuki–Miyaura cross-coupling reaction in presence of MNPs–MIC–Pd nanomagnetic catalyst^a

Entry	Base	Solvent	Temperature (°C)	Time (h)	Yield (%) ^b
1	Na ₂ CO ₃	EtOH	RT	2.0	68
2	Na ₂ CO ₃	H ₂ O	RT	2.0	55
3	Na ₂ CO ₃	EtOH:H ₂ O (1:1)	RT	0.16	94
4	Na ₂ CO ₃	CH ₃ CN	RT	3.0	Trace
5	Na ₂ CO ₃	MeOH	RT	2.5	58
6	Na ₂ CO ₃	THF	RT	3.0	Trace
7	Na ₂ CO ₃	Toluene	RT	2.0	Trace
8	Na ₂ CO ₃	DCM	RT	3.0	Trace
9	Na ₂ CO ₃	DMF	RT	2.0	Trace
10	Na ₂ CO ₃	IPA	RT	1.5	Trace
11	K ₂ CO ₃	EtOH:H ₂ O (1:1)	RT	0.16	92
12	NaOH	EtOH:H ₂ O (1:1)	RT	1.0	84
13	KOH	EtOH:H ₂ O (1:1)	RT	1.5	81
14	Et ₃ N	EtOH:H ₂ O (1:1)	RT	2.0	85
15	Na ₃ PO ₄ ·12H ₂ O	EtOH:H ₂ O (1:1)	RT	3.0	80
16	CS ₂ CO ₃	EtOH:H ₂ O (1:1)	RT	2.0	78
17	KF	EtOH:H ₂ O (1:1)	RT	2.0	Trace
18	Na ₂ CO ₃	EtOH:H ₂ O (1:1)	0	4.0	38
19	Na ₂ CO ₃	EtOH:H ₂ O (1:1)	15	4.0	52
20	Na ₂ CO ₃	EtOH:H ₂ O (1:1)	40	0.16	94
21	Na ₂ CO ₃	EtOH:H ₂ O (1:1)	50	0.16	94
22	Na ₂ CO ₃	EtOH:H ₂ O (1:1)	60	0.16	93
23	Na ₂ CO ₃	EtOH:H ₂ O (1:1)	70	0.16	94
24	Na ₂ CO ₃	EtOH:H ₂ O (1:1)	RT	0.08	82
25	Na ₂ CO ₃	EtOH:H ₂ O (1:1)	RT	0.33	94
26	Na ₂ CO ₃	EtOH:H ₂ O (1:1)	RT	0.5	94
27	Na ₂ CO ₃	EtOH:H ₂ O(1:1)	RT	0.66	94
28	Na ₂ CO ₃	EtOH:H ₂ O (1:1)	RT	0.83	94
29	Na ₂ CO ₃	EtOH:H ₂ O (1:1)	RT	1.0	94

^aReaction conditions: 4-bromoanisole (1.0 mmol), phenylboronic acid (1.1 mmol), MNPs–MIC–Pd nanomagnetic catalyst (0.025 mol% Pd with respect to aryl halide), base (2.2 mmol) and solvent (10 ml) in air.

^bIsolated yield after separation by column chromatography.

3.4 | Effect of base on Suzuki-Miyaura cross-coupling reaction

In the outset, the effectiveness of different bases such as K_2CO_3 , Na_2CO_3 , $NaOH$, KOH , Et_3N , $Na_3PO_4 \cdot 12H_2O$, Cs_2CO_3 and KF were examined in model Suzuki-Miyaura cross-coupling reaction at room temperature using EtOH:H₂O (1:1) solvent system and MNPs-MIC-Pd nanomagnetic catalyst (0.025 mol% Pd with respect to aryl halide) (Table 1). Na_2CO_3 and K_2CO_3 bases gave excellent yield (Table 1, entries 3 and 11) while $NaOH$, KOH , Et_3N , $Na_3PO_4 \cdot 12H_2O$ and Cs_2CO_3 resulted in lesser conversion (Table 1, entries 12–16). However, using base KF led to low conversion (Table 1, entry 17).

3.5 | Effect of solvent on Suzuki-Miyaura cross-coupling reaction

The efficiency of a variety of solvents such as EtOH, H₂O, EtOH:H₂O (1:1), CH₃CN, methanol (MeOH), THF, Toluene, DCM, DMF and isopropanol (IPA) were studied in model Suzuki-Miyaura cross-coupling reaction at room temperature using MNPs-MIC-Pd nanomagnetic catalyst (0.025 mol% Pd with respect to aryl halide). The results indicated that reaction went well with polar solvents such as EtOH, H₂O, EtOH:H₂O (1:1) and MeOH (Table 1, entries 1–3 and 5) except with CH₃CN, DCM and DMF (Table 1, entries 4, 8 and 9). Surprisingly, MNPs-MIC-Pd nanomagnetic catalyst did not show any catalytic activity in THF, toluene and isopropanol solvents (Table 1, entries 6, 7 and 10).

3.6 | Effect of temperature on Suzuki-Miyaura cross-coupling reaction

To investigate the catalytic activity of MNPs-MIC-Pd nanomagnetic catalyst towards Suzuki-Miyaura cross-coupling reaction at varying temperatures, the model reaction was carried out at different temperatures as

depicted in Table 1. High conversion was observed at room temperature (Table 1, entry 3). At lower reaction temperatures (0 °C and 15 °C) yield decreases even after long reaction times (Table 1, entries 18 and 19). At higher reaction temperatures (40 °C, 50 °C, 60 °C and 70 °C) yield did not improve (Table 1, entries 20–23). Therefore, all reactions were carried out at room temperature.

3.7 | Effect of time on Suzuki-Miyaura cross-coupling reaction

To know the effect of time, the model Suzuki-Miyaura cross-coupling reaction was carried out at different time intervals with MNPs-MIC-Pd nanomagnetic catalyst as depicted in Table 1. Initially, at 5 min 82% yield was obtained (Table 1, entry 24) and subsequently, at 10 min a higher conversion or maximum yield was obtained (Table 1, entry 3). Further increase in time beyond 20 min does not improve the yield (Table 1, entries 25–29). Hence, 10 min is the optimal reaction time for the model Suzuki-Miyaura cross-coupling reaction.

3.8 | Effect of catalyst ratio on Suzuki-Miyaura cross-coupling reaction

The quantity of catalyst plays a major role in Suzuki-Miyaura cross-coupling reactions. Hence, in order to find out the suitable quantity of the MNPs-MIC-Pd nanomagnetic catalyst, various catalyst ratios 0.02, 0.025, 0.03, 0.035, 0.04 and 0.045 mol% Pd were used in the model Suzuki-Miyaura cross-coupling reaction (Table 2). A maximum yield was obtained using 0.025 mol% Pd of the MNPs-MIC-Pd nanomagnetic catalyst (Table 2, entry 2). Further, use of higher quantities of the MNPs-MIC-Pd nanomagnetic catalyst (0.03, 0.035, 0.04 and 0.045 mol% Pd) does not increase the conversion (Table 2, entries 3–6). Hence, 0.025 mol% Pd of MNPs-MIC-Pd nanomagnetic catalyst is best catalyst quantity for model Suzuki-Miyaura cross-coupling reaction (Table 2, entry 2).

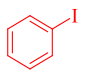
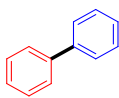
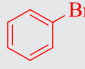
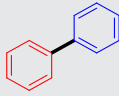
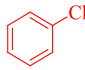
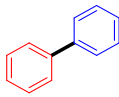
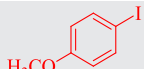
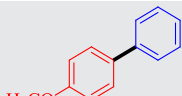
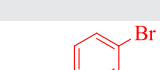
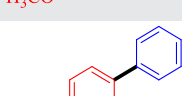
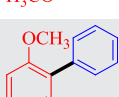

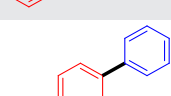

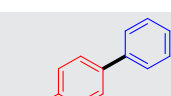
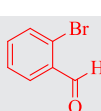
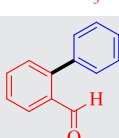

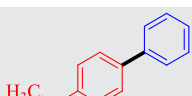
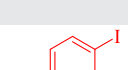
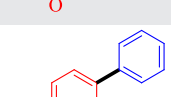
TABLE 2 Suzuki-Miyaura cross-coupling in presence of MNPs-MIC-Pd nanomagnetic catalyst with various catalyst ratios for the model reaction^a

Entry	Base	Solvent	Temperature (°C)	Pd (mol %)	Yield (%) ^b
1	Na_2CO_3	EtOH:H ₂ O (1:1)	RT	0.02	73
2	Na_2CO_3	EtOH:H₂O (1:1)	RT	0.025	94
3	Na_2CO_3	EtOH:H ₂ O (1:1)	RT	0.03	94
4	Na_2CO_3	EtOH:H ₂ O (1:1)	RT	0.035	94
5	Na_2CO_3	EtOH:H ₂ O (1:1)	RT	0.04	94
6	Na_2CO_3	EtOH:H ₂ O (1:1)	RT	0.045	94

^aReaction conditions: 4-bromoanisole (1.0 mmol), phenylboronic acid (1.1 mmol), Na_2CO_3 (2.2 mmol) and EtOH:H₂O (1:1) 10 ml in air.

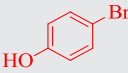
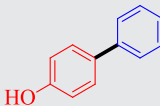
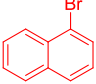
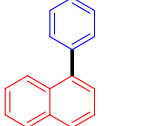
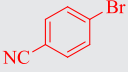
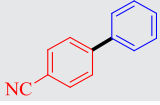
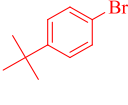
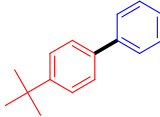
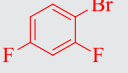
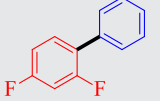
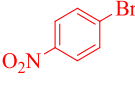
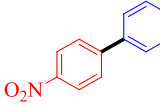
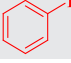
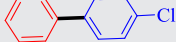
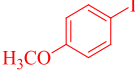
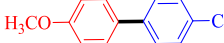
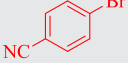

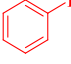
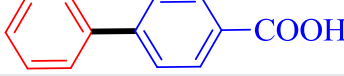
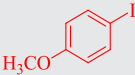
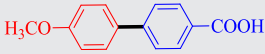
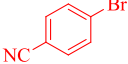
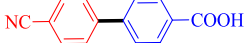
^bIsolated yield after separation by column chromatography.

TABLE 3 Suzuki-Miyaura cross-coupling reactions between aryl halides with arylboronic acids catalyzed by MNPs-MIC-Pd nanomagnetic catalyst^a

$\text{R}^1\text{-C}_6\text{H}_4\text{-X} + (\text{HO})_2\text{B-C}_6\text{H}_4\text{-R}^2 \xrightarrow[\text{Na}_2\text{CO}_3]{\text{MNPs-MIC-Pd, EtOH:H}_2\text{O (1:1), RT}} \text{R}^1\text{-C}_6\text{H}_4\text{-C}_6\text{H}_4\text{-R}^2$				
Entry	Aryl halide	Product	Time (h)	Yield (%) ^b
1			0.08	99
2			0.08	98
3			0.5	84
4			0.08	98
5			0.16	94
6			0.08	95
7			0.08	98
8			0.16	98
9			0.16	94
^c 10			24	64
^c 11			24	65
^c 12			24	89
13			0.16	92

(Continues)

TABLE 3 (Continued)

$\text{R}^1\text{-C}_6\text{H}_4\text{-X} + (\text{HO})_2\text{B-C}_6\text{H}_4\text{-R}^2 \xrightarrow[\text{Na}_2\text{CO}_3]{\text{MNP}s\text{-MIC-Pd, EtOH:H}_2\text{O (1:1), RT}} \text{R}^1\text{-C}_6\text{H}_4\text{-C}_6\text{H}_4\text{-R}^2$				
Entry	Aryl halide	Product	Time (h)	Yield (%) ^b
14			0.33	90
^c 15			24	68
16			0.5	92
17			0.08	98
18			0.16	98
19			1.0	96
20			0.16	95
21			0.16	85
22			1.0	81
23			0.16	88
24			0.16	83
25			1.0	80

^aReaction conditions: aryl halide (1.0 mmol), arylboronic acid (1.1 mmol), MNPs-MIC-Pd nanomagnetic catalyst (0.025 mol% Pd with respect to aryl halide), Na₂CO₃ (2.2 mmol) and EtOH:H₂O (1:1) (10 ml) in air.

^bIsolated yield after separation by column chromatography; average of two runs.

^cReactions were carried out at 70 °C.

3.9 | Suzuki-Miyaura cross-coupling reactions of different aryl halides

To investigate the scope and generality of the Suzuki-Miyaura cross-coupling reaction we studied the reaction

of arylboronic acids with a range of aryl halides under the aforementioned optimized conditions and the results are summarized in Table 3. The presented Suzuki-Miyaura cross-coupling reaction procedure is very simple, convenient and has the capability to bear a wide variety

of functional groups. All the aryl bromides with electron-withdrawing or electron releasing groups react with arylboronic acids to afford the corresponding products in high yields (Table 3, entries 2, 5, 8, 9, 12, 14–19, 22 and 25) except 2-bromobenzaldehyde (Table 3, entry 10) and 4-bromobenzaldehyde (Table 3, entry 11). Hence, it can be concluded that the reaction yield was not dependent on the electronic properties of the substituent on the aryl bromides. Conversely, aryl iodides gave excellent yields as expected (Table 3, entries 1, 4, 6, 7, 13, 20, 21, 23 and 24). On the other hand, aryl chloride gave lesser yield compared with their bromide and iodide counter parts under the same reaction conditions

(Table 3, entry 3) as the C–Cl bond strength is high due to the stronger 2s–3p interaction. These results indicated that our newly prepared MNPs-MIC-Pd nanomagnetic catalyst is good catalyst for Suzuki–Miyaura cross-coupling reaction. Additionally, MNPs-MIC-Pd nanomagnetic catalyst was further studied towards selectivity through conducting the Suzuki–Miyaura cross-coupling reaction using the optimized reaction conditions in the absence of aryl bromide. The biphenyl homo-coupled product was negligible even after longer reaction time. Hence, it is concluded that our newly synthesized MNP-MIC-Pd nanomagnetic catalyst is highly selective.

TABLE 4 Recyclability of MNPs-MIC-Pd nanomagnetic catalyst in Suzuki-Miyaura cross coupling reactions of bromobenzene and phenylboronic acid^a

Entry	Base	Solvent	Temperature (°C)	Catalyst run	Yield (%) ^b
1	Na ₂ CO ₃	EtOH:H ₂ O (1:1)	RT	Fresh	98
2	Na ₂ CO ₃	EtOH:H ₂ O (1:1)	RT	1 st recycle	98
3	Na ₂ CO ₃	EtOH:H ₂ O (1:1)	RT	2 nd recycle	98
4	Na ₂ CO ₃	EtOH:H ₂ O (1:1)	RT	3 rd recycle	98
5	Na ₂ CO ₃	EtOH:H ₂ O (1:1)	RT	4 th recycle	98
6	Na ₂ CO ₃	EtOH:H ₂ O (1:1)	RT	5 th recycle	97
7	Na ₂ CO ₃	EtOH:H ₂ O (1:1)	RT	6 th recycle	97
8	Na ₂ CO ₃	EtOH:H ₂ O (1:1)	RT	7 th recycle	97
9	Na ₂ CO ₃	EtOH:H ₂ O (1:1)	RT	8 th recycle	96
10	Na ₂ CO ₃	EtOH:H ₂ O (1:1)	RT	9 th recycle	96
11	Na ₂ CO ₃	EtOH:H ₂ O (1:1)	RT	10 th recycle	95

^aReaction conditions: bromobenzene (1.0 mmol), phenylboronic acid (1.1 mmol), MNPs-MIC-Pd nanomagnetic catalyst (0.025 mol% Pd with respect to aryl halide), Na₂CO₃ (2.2 mmol) and EtOH:H₂O (1:1) (10 ml) in air.

^bIsolated yield after separation by column chromatography.

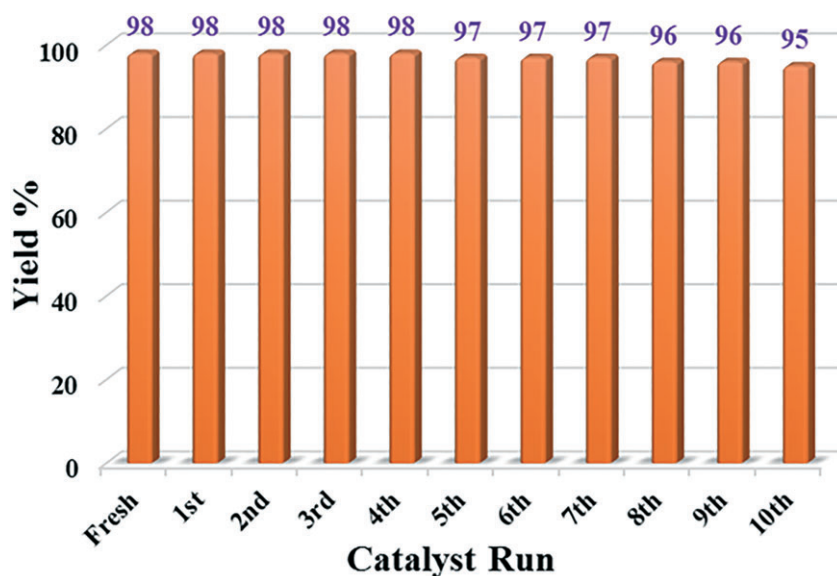
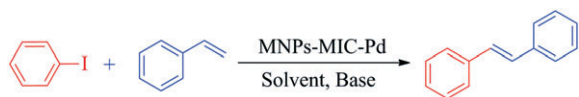


FIGURE 11 The recycling efficiency of MNPs-MIC-Pd nanomagnetic catalyst in Suzuki-Miyaura cross-coupling reaction of bromobenzene and phenylboronic acid

3.10 | Recyclability of the MNPs-MIC-Pd nanomagnetic catalyst in Suzuki-Miyaura cross-coupling reactions

For convenient applications of a heterogeneous catalyst, recyclability of the catalyst is a very important factor. To explain this matter, catalytic recyclability experiments were carried out for the Suzuki-Miyaura cross-coupling reaction of bromobenzene with phenylboronic acid. After completion of Suzuki-Miyaura cross-coupling reactions, MNPs-MIC-Pd nanomagnetic catalyst was separated by applying an external magnet and washed thoroughly with H₂O (2 x 10 ml), followed by EtOH (2 x 10 ml) and dried at 45 °C overnight. Then the same MNPs-MIC-Pd nanomagnetic catalyst was reused for next cycle without any further purification. Recycling efficiency of MNPs-MIC-Pd nanomagnetic catalyst is tabulated in Table 4. The recyclability of MNPs-MIC-Pd nanomagnetic catalyst



SCHEME 3 Mizoroki-Heck cross-coupling reaction of iodobenzene with styrene in presence of MNPs-MIC-Pd nanomagnetic catalyst

revealed that catalyst can be reused for minimum ten times in Suzuki-Miyaura cross-coupling reactions without loss of its catalytic activity (Figure 11) (Table 4, entries 1–11). After ten cycles, recovered MNPs-MIC-Pd nanomagnetic catalyst was further characterized by FESEM and FT-IR spectroscopy. The FESEM image (Figure 5b) and FT-IR spectra (Figure 2b) of reused MNPs-MIC-Pd nanomagnetic catalyst indicated that there is no change in surface morphology and chemical composition. This result exhibits the high stability of the MNPs-MIC-Pd nanomagnetic catalyst.

3.11 | Catalytic activity of MNPs-MIC-Pd nanomagnetic catalyst in Mizoroki-Heck cross-coupling reactions

In the second part of our study, we explored the applicability of MNPs-MIC-Pd nanomagnetic catalyst in the Mizoroki-Heck cross-coupling reaction of aryl halides with styrene and *tert*-butyl acrylate. In order to optimize the reaction conditions, we have selected the cross-coupling of iodobenzene with styrene as a model reaction (Scheme 3). The reaction conditions were optimized through a series of reactions as listed in Table 5. In

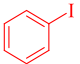
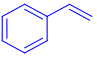
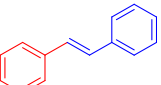
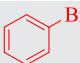
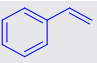
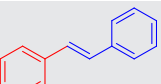
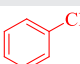
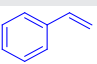
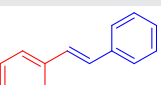
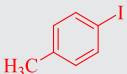
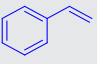
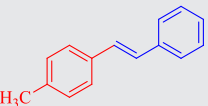
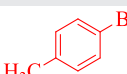
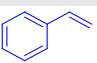
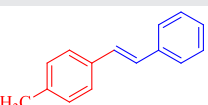
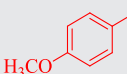
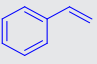
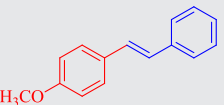
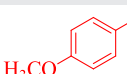
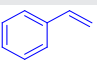
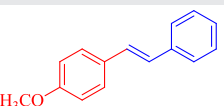
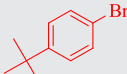
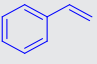
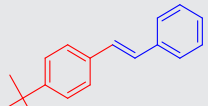
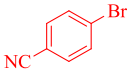
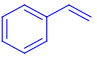
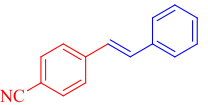
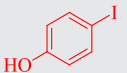
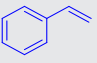
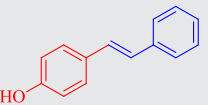
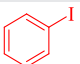
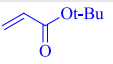
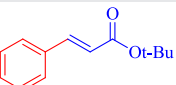
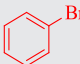
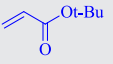
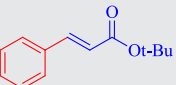
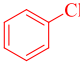
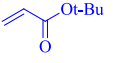
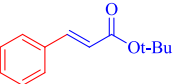
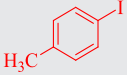
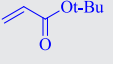
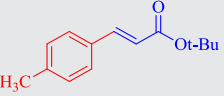
TABLE 5 Optimization of reaction conditions for the model Mizoroki-Heck cross-coupling reaction in presence of MNPs-MIC-Pd nanomagnetic catalyst^a

Entry	Solvents	Base	Pd (mol %)	Temperature (°C)	Time (h)	Yield(%) ^b
1	H ₂ O	Na ₂ CO ₃	0.05	RT	2.0	-
2	EtOH	Na ₂ CO ₃	0.05	RT	2.0	-
3	EtOH:H ₂ O(1:1)	Na ₂ CO ₃	0.05	RT	1.5	95
4	EtOH:H ₂ O(1:1)	Na ₂ CO ₃	0.05	70	0.5	95
5	EtOH:H ₂ O(1:1)	Na ₂ CO ₃	0.05	RT	0.16	81
6	EtOH:H ₂ O(1:1)	Na ₂ CO ₃	0.05	RT	0.33	85
7	EtOH:H ₂ O(1:1)	K ₂ CO ₃	0.05	RT	0.33	85
8	EtOH:H ₂ O(1:1)	Na ₂ CO ₃	0.05	RT	0.5	89
9	EtOH:H₂O(1:1)	Na₂CO₃	0.05	RT	1.0	95
10	EtOH:H ₂ O(1:1)	K ₂ CO ₃	0.05	RT	0.5	85
11	EtOH:H ₂ O(1:1)	K ₂ CO ₃	0.05	RT	1.0	88
12	EtOH:H ₂ O(1:1)	Na ₂ CO ₃	0.025	RT	1.0	74
13	EtOH:H ₂ O(1:1)	Na ₂ CO ₃	0.075	RT	1.0	95
14	EtOH:H ₂ O(1:1)	NaOH	0.05	RT	1.0	75
15	EtOH:H ₂ O(1:1)	CS ₂ CO ₃	0.05	RT	1.0	53
16	DMF	Na ₂ CO ₃	0.05	RT	0.5	61
17	MeOH	Na ₂ CO ₃	0.05	RT	0.5	-

^aReaction conditions: iodobenzene (1.0 mmol), styrene (1.2 mmol), MNPs-MIC-Pd nanomagnetic catalyst (0.05 mol % Pd with respect to aryl halide), base (2.0 mmol) and solvent (10 ml) in air.

^bIsolated yield after separation by column chromatography.

TABLE 6 Mizoroki-Heck cross-coupling of different aryl halides with alkenes in the presence of MNPs-MIC-Pd nanomagnetic catalyst^a

$\text{R}_1\text{-C}_6\text{H}_4\text{-X} + \text{R}_2\text{-CH=CH}_2 \xrightarrow[\text{EtOH:H}_2\text{O(1:1)}]{\text{MNPs-MIC-Pd, RT, Na}_2\text{CO}_3} \text{R}_1\text{-C}_6\text{H}_4\text{-CH=CH-R}_2$					
Entry	Aryl halide	Alkene	Product	Time (h)	Yield (%) ^b
1				1.0	95
2				1.5	91
3				6.0	82
4				24	92
5				24	90
6				6	58
7				6	52
8				24	Trace
9				16	82
10				24	Trace
11				1.0	91
12				2.0	88
13				5.0	78
14				24	90

(Continues)

TABLE 6 (Continued)

$\text{R}_1\text{-C}_6\text{H}_4\text{-X} + \text{R}_2\text{-CH=CH}_2 \xrightarrow[\text{EtOH:H}_2\text{O}(1:1)]{\text{MNP s-MIC-Pd, RT, Na}_2\text{CO}_3}$					
Entry	Aryl halide	Alkene	Product	Time (h)	Yield (%) ^b
15				24	84
16				16	73

^aReaction conditions: aryl halide (1.0 mmol), alkene (1.2 mmol), MNPs-MIC-Pd nanomagnetic catalyst (0.05 mol% Pd with respect to aryl halide), Na₂CO₃ (2.0 mmol) and EtOH:H₂O (1:1) 10 ml in air.

^bIsolated yield after separation by column chromatography; average of two runs.

order to choose the reaction solvent, various solvents (H₂O, EtOH, EtOH:H₂O (1:1), DMF and MeOH) and amounts of MNPs-MIC-Pd nanomagnetic catalyst were examined. The good results were obtained in EtOH:H₂O (1:1) solvent mixture using 0.05 mol% Pd of MNPs-MIC-Pd nanomagnetic catalyst (Table 5, entry 9). In addition, the model reaction was examined using numerous bases such as Na₂CO₃, K₂CO₃, NaOH and CS₂CO₃ and the good results were observed using two equivalents of Na₂CO₃ (Table 5, entry 9). Furthermore, the effect of temperature was studied and found out that the reaction proceeded well at room temperature itself (Table 5, entry 9).

After the optimization of the reaction conditions, a variety of aryl halides having numerous functional groups were reacted with styrene and *tert*-butyl acrylate under the optimized conditions and the results are summarized in Table 6. All the aryl bromides and aryl iodides having electron-withdrawing or electron-releasing groups reacted with olefins to afford the corresponding products in high yields (Table 6, entries 1, 2, 4–7, 9, 11, 12 and 14–16) except 1-bromo-4-*tert*-butylbenzene (Table 6, entry 8) and 4-iodophenol (Table 6, entry 10). However, aryl chlorides gave lower yields when compared to their iodide and bromide counterparts (Table 6, entries 3 and 13). Therefore, obtained results concluded that MNPs-MIC-Pd nanomagnetic catalyst is an efficient catalyst towards Mizoroki–Heck cross-coupling reactions for the synthesis of various substituted olefins.

3.12 | Recyclability of the MNPs-MIC-Pd nanomagnetic catalyst in Mizoroki–Heck cross-coupling reactions

The recyclability of catalyst is an important feature required for a catalyst for commercial applications. To

investigate this issue, the recyclability of the MNPs-MIC-Pd nanomagnetic catalyst was examined for the cross-coupling of iodobenzene with styrene under the optimized conditions. After the completion of the reaction, the MNPs-MIC-Pd nanomagnetic catalyst was easily separated from the products using an external magnet and used in the next round of reaction after washing with H₂O (2 x 10 ml) followed by EtOH (2 x 10 ml) and dried at 45 °C. As shown in Figure 12, the MNPs-MIC-Pd nanomagnetic catalyst used over five runs without any significant loss of activity or palladium leaching. From sixth recycle onwards, a decrease in catalytic activity was observed (Table 7). The FESEM image and FT-IR spectrum of five times recycled MNPs-MIC-Pd nanomagnetic catalyst was recorded. No change in the morphology was observed through the FESEM image (Figure 5c) after recycling up to five times which is further confirmed by the FT-IR spectrum (Figure 2c) which shows that the MNPs-MIC-Pd nanomagnetic catalyst is intact after recycling.

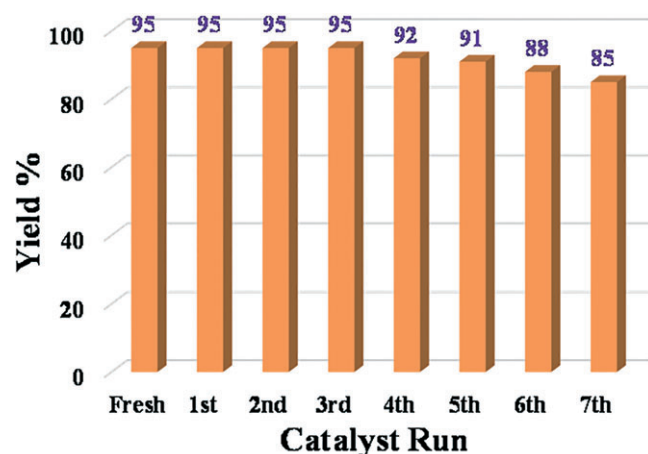


FIGURE 12 Recycling efficiency of MNPs-MIC-Pd nanomagnetic catalyst in the reaction of iodobenzene and styrene

TABLE 7 Recyclability of MNPs-MIC-Pd nanomagnetic catalyst in Mizoroki–Heck cross coupling reactions of iodobenzene with styrene^a

Entry	Base	Solvent	Temperature (°C)	Catalyst Run	Yield(%) ^b
1	Na ₂ CO ₃	EtOH:H ₂ O (1:1)	RT	Fresh	95
2	Na ₂ CO ₃	EtOH:H ₂ O (1:1)	RT	1 st recycle	95
3	Na ₂ CO ₃	EtOH:H ₂ O (1:1)	RT	2 nd recycle	95
4	Na ₂ CO ₃	EtOH:H ₂ O (1:1)	RT	3 rd recycle	95
5	Na ₂ CO ₃	EtOH:H ₂ O (1:1)	RT	4 th recycle	92
6	Na ₂ CO ₃	EtOH:H ₂ O (1:1)	RT	5 th recycle	91
7	Na ₂ CO ₃	EtOH:H ₂ O (1:1)	RT	6 th recycle	88
8	Na ₂ CO ₃	EtOH:H ₂ O (1:1)	RT	7 th recycle	85

^aReaction conditions: iodobenzene (1.0 mmol), styrene (1.2 mmol), MNPs-MIC-Pd nanomagnetic catalyst (0.05 mol% Pd with respect to aryl halide), Na₂CO₃ (2.0 mmol) and EtOH:H₂O (1:1) 10 ml in air.

^bIsolated yield after separation by column chromatography; average of two runs.

3.13 | Catalyst leaching study

One problem that should be addressed when using heterogeneous catalysts is metal leaching in to the reaction solution. The leaching of palladium from catalyst was studied for the model Suzuki–Miyaura cross-coupling reaction in the optimized reaction conditions. The MNPs-MIC-Pd nanomagnetic catalyst was recovered after 5 min by an external magnet and the same reaction was further continued for more than 2 hr and the reaction was monitored by TLC. Further conversion was not observed and the isolated yield was 82%. After recovery of MNPs-MIC-Pd nanomagnetic catalyst from reaction

mixture, ICP-AES analysis was carried out for both the recovered catalyst as well as reaction mixture and found that the Pd content in MNPs-MIC-Pd nanomagnetic catalyst was 4.82% (w/w) and that in the reaction mixture was 0.000419% (w/w) (4.19 ppm). This confirms that the leaching of Pd from the MNPs-MIC-Pd nanomagnetic catalyst is negligible in the reaction possibly because of the specific design of nanomagnetic catalyst.

3.14 | Comparison of catalysts

Comparison of catalytic activity of MNPs-MIC-Pd nanomagnetic catalyst with previously reported catalysts

TABLE 8 Comparison of results in Suzuki–Miyaura cross-coupling reaction between bromobenzene and phenylboronic acid of other reported catalysts with the MNPs-MIC-Pd nanomagnetic catalyst

Entry	Catalyst	Solvent	Temp. (°C)	Time (h)	Yield (%)	Ref.
1	Click-catalyst A	EtOH:H ₂ O (1:1)	70	0.75	90	[47]
2	Fe ₃ O ₄ @SiO ₂ -EDTA-Pd	EtOH:H ₂ O (1:1)	70	2	97	[48]
3	Si-IL@Pd(0)NPs	EtOH:H ₂ O (1:1)	50	4	95	[49]
4	Pd _{np} @MNP	EtOH:H ₂ O (1:1)	60	4	97	[43]
5	Fe ₃ O ₄ /SiO ₂ -NH ₂ /SA/Pd	Toluene	75	1	85	[50]
6	NHC-Pd Complex	DMF:H ₂ O (1:1)	50	6	95	[51]
7	P-PdNPs/CMK-3	EtOH:H ₂ O (1:1)	40	0.5	98	[52]
8	AA-PdNPs/CMK-3	EtOH:H ₂ O (1:1)	40	0.5	93	[52]
9	Pd/IL-NH ₂ /SiO ₂ /Fe ₃ O ₄	EtOH:H ₂ O (1:1)	25	5	87	[53]
10	SB-Pd@MNPs	EtOH:H ₂ O (1:1)	RT	0.5	85	[40]
11	MNPs@SB-Pd	EtOH:H ₂ O (1:1)	RT	3	69	[41]
12	NHC-Pd@MNPs	EtOH:H ₂ O (1:1)	70	1	95	[38]
13	NO ₂ -NHC-Pd@Fe ₃ O ₄	EtOH:H ₂ O (1:1)	RT	2	95	[39]
14	MNP-MCP-Pd	EtOH:H ₂ O (1:1)	RT	0.08	98	Present work

TABLE 9 Comparison of results in Mizoroki–Heck cross-coupling reaction between iodobenzene and styrene of other reported catalysts with the MNPs-MIC-Pd nanomagnetic catalyst

Entry	Catalyst	Solvent	Temp. (°C)	Time (h)	Yield (%)	Ref.
1	SiO ₂ @Fe ₃ O ₄ -Pd	DMF	100	8	95	[54]
2	Catalyst	DMF	90	24	100	[55]
3	MNP@NHC-Pd	DMF	140	3	96	[56]
4	Pd-MNPSS	H ₂ O	100	4	89	[57]
5	Pd-imine@MNPs/Cs	H ₂ O	RT	0.33	75	[58]
6	Catalyst	NMP	140	15	97	[59]
7	Pd-Catalyst	DMF	120	0.16	98	[60]
8	NO ₂ -NHC-Pd@Fe ₃ O ₄	MeCN	80	5	96	[39]
9	MNPs-MCP-Pd	EtOH:H₂O (1:1)	RT	1	95	Present work

for Suzuki-Miyaura and Mizoroki-Heck cross-coupling reactions are presented in Table 8 and Table 9 respectively. Comparison of the results shows that our new MNPs-MIC-Pd nanomagnetic catalyst is extremely active catalyst towards both Suzuki-Miyaura and Mizoroki-Heck cross-coupling reactions under mild reaction conditions. Also, MNPs-MIC-Pd nanomagnetic catalyst is superior in terms of non-toxicity, price, stability and ease of separation than the previously reported ones. Furthermore, the recyclability MNPs-MIC-Pd nanomagnetic catalyst is easier and rapid than those of other reported catalysts.^[38–41,43,47–60]

4 | CONCLUSION

An efficient heterogeneous MNPs-MIC-Pd nanomagnetic catalyst was successfully synthesised and characterised through various spectroscopic and microscopic techniques. The MNPs-MIC-Pd nanomagnetic catalyst exhibits excellent catalytic activity towards both Suzuki-Miyaura and Mizoroki–Heck cross-coupling reactions. The main advantages of MNPs-MIC-Pd nanomagnetic catalyst are highly active, selective, eco-friendly, cost effective and easy recovery by an external magnet from the reaction mixture. Moreover, recovered MNPs-MIC-Pd nanomagnetic catalyst can be used at least ten times in Suzuki-Miyaura and five times in Mizoroki–Heck cross-coupling reactions. Furthermore, MNPs-MIC-Pd nanomagnetic catalyst can be used as nanomagnetic catalyst for many other organic transformations such as Sonogashira-Hagihara and Hiyama cross-coupling, C-H activation, oxidation and reduction reactions.

ACKNOWLEDGEMENTS

The authors thank DST-SERB, India (YSS/2015/000010), DST-Nanomission, India (SR/NM/NS-20/2014), and Jain University, India for financial support.

ORCID

Siddappa A. Patil  <https://orcid.org/0000-0002-2855-5302>

REFERENCES

- [1] Z. Zarnegar, J. Safari, *New J. Chem.* **2014**, *38*, 4555.
- [2] A. Corma, H. Garcia, *Top. Catal.* **2008**, *48*, 8.
- [3] C. Coperet, M. Chabanas, R. Petroff Saint-Arroman, J. M. Basset, *Angew. Chem. Int. Ed.* **2003**, *42*, 156.
- [4] V. Polshettiwar, R. S. Varma, *Green Chem.* **2010**, *12*, 743.
- [5] S. Shylesh, V. Schünemann, W. R. Thiel, *Angew. Chem. Int. Ed.* **2010**, *49*, 3428.
- [6] A. J. Arduengo III, R. L. Harlow, M. Kline, *J. Am. Chem. Soc.* **1991**, *113*, 361.
- [7] W. Wang, F. Wang, M. Shi, *Organometallics* **2010**, *29*, 928.
- [8] M. Alcarazo, T. Stork, A. Anoop, W. Thiel, A. Fürstner, *Angew. Chem. Int. Ed.* **2010**, *49*, 2542.
- [9] G. Buscemi, M. Basato, A. Biffis, A. Gennaro, A. A. Isse, M. M. Natile, C. Tubaro, *J. Organomet. Chem.* **2010**, *695*, 2359.
- [10] P. de Frémont, N. Marion, S. P. Nolan, *Coord. Chem. Rev.* **2009**, *253*, 862.
- [11] S. Diez-Gonzalez, N. Marion, S. P. Nolan, *Chem. Rev.* **2009**, *109*, 3612.
- [12] O. Schuster, L. Yang, H. G. Raubenheimer, M. Albrecht, *Chem. Rev.* **2009**, *109*, 3445.
- [13] M. Poyatos, J. A. Mata, E. Peris, *Chem. Rev.* **2009**, *109*, 3677.
- [14] D. Enders, O. Niemeier, A. Henseler, *Chem. Rev.* **2007**, *107*, 5606.
- [15] E. C. Hurst, K. Wilson, I. J. Fairlamb, V. Chechik, *New J. Chem.* **2009**, *33*, 1837.
- [16] P. Lara, O. Rivada-Wheelaghan, S. Conejero, R. Poteau, K. Philippot, B. Chaudret, *Angew. Chem.* **2011**, *123*, 12286.
- [17] J. Vignolle, T. D. Tilley, *Chem. Commun.* **2009**, *46*, 7230.
- [18] R. H. Crabtree, *Coord. Chem. Rev.* **2013**, *257*, 755.
- [19] K. O. Marichev, S. A. Patil, A. Bugarin, *Tetrahedron* **2018**, *74*, 2523.
- [20] P. Mathew, A. Neels, M. Albrecht, *J. Am. Chem. Soc.* **2008**, *130*, 13534.

- [21] R. Saravanakumar, V. Ramkumar, S. Sankararaman, *Organometallics* **2011**, *30*, 1689.
- [22] G. Guisado-Barrios, J. Bouffard, B. Donnadiu, B. Bertrand, *Angew. Chem. Int.* **2010**, *49*, 4759.
- [23] L. Yin, J. Liebscher, *Chem. Rev.* **2007**, *107*, 133.
- [24] N. T. Phan, M. Van Der Sluys, C. W. Jones, *Adv. Synth. Catal.* **2006**, *348*, 609.
- [25] J.-P. Corbet, G. Mignani, *Chem. Rev.* **2006**, *106*, 2651.
- [26] J. Hassan, M. Sevignon, C. Gozzi, E. Schulz, M. Lemaire, *Chem. Rev.* **2002**, *102*, 1359.
- [27] J. K. Belardi, G. C. Micalizio, *Angew. Chem. Int. Ed.* **2008**, *47*, 4005.
- [28] Y. Jia, M. Bois-Choussy, J. Zhu, *Angew. Chem. Int. Ed.* **2008**, *47*, 4167.
- [29] J. A. Burlison, L. Neckers, A. B. Smith, A. Maxwell, B. S. Blagg, *J. Am. Chem. Soc.* **2006**, *128*, 15529.
- [30] K. Nicolaou, H. Li, C. N. Boddy, J. M. Ramanjulu, T. Y. Yue, S. Natarajan, X. J. Chu, S. Bräse, F. Rübsam, *Chem. – Eur. J.* **1999**, *5*, 2584.
- [31] S. P. Stanforth, *Tetrahedron* **1998**, *54*, 263.
- [32] J. P. Knowles, A. Whiting, *Org. Biomol. Chem.* **2007**, *5*, 31.
- [33] S. Inomata, H. Hiroki, T. Terashima, K. Ogata, S. Fukuzawa, *Tetrahedron* **2011**, *67*, 7263.
- [34] E. C. Keske, O. V. Zenkina, R. Wang, C. M. Crudden, *Organometallics* **2012**, *31*, 6215.
- [35] J. Lorkowski, P. Zak, M. Kubicki, C. Pietraszuk, D. Jedrzkiewicz, J. Ejfler, *New J. Chem.* **2018**, *42*, 10134.
- [36] T. Mitsui, M. Sugihara, Y. Tokoro, S. Fukuzawa, *Tetrahedron* **2015**, *71*, 1509.
- [37] R. Rahimi, A. Maleki, S. Maleki, A. Morsali, M. J. Rahimi, *Solid State Sci.* **2014**, *28*, 9.
- [38] K. Vishal, B. D. Fahlman, B. Sasidhar, S. A. Patil, S. A. Patil, *Catal. Lett.* **2017**, *147*, 900.
- [39] V. Kandathil, B. D. Fahlman, B. Sasidhar, S. A. Patil, S. A. Patil, *New J. Chem.* **2017**, *41*, 9531.
- [40] K. Manjunatha, T. S. Koley, V. Kandathil, R. B. Dateer, G. Balakrishna, B. Sasidhar, S. A. Patil, S. A. Patil, *Appl. Organomet. Chem.* **2018**, *32*, 4266.
- [41] V. Kandathil, T. S. Koley, K. Manjunatha, R. B. Dateer, R. S. Keri, B. Sasidhar, S. A. Patil, S. A. Patil, *Inorg. Chim. Acta* **2018**, *478*, 195.
- [42] V. Kandathil, R. B. Dateer, B. Sasidhar, S. A. Patil, S. A. Patil, *Catal. Lett.* **2018**, *1*.
- [43] Q. Zhang, H. Su, J. Luo, Y. Wei, *Catal. Sci. Technol.* **2013**, *3*, 235.
- [44] A. S. Singh, R. S. Shelkar, J. M. Nagarkar, *Catal. Lett.* **2015**, *145*, 723.
- [45] J. Y. Kim, K. Park, S. Y. Bae, G. C. Kim, S. Lee, H. C. Choi, *J. Mater. Chem.* **2011**, *2*, 5999.
- [46] S. Santra, P. Ranjan, P. Bera, P. Ghosh, S. K. Mandal, *RSC Adv.* **2012**, *2*, 7523.
- [47] A. R. Hajipour, F. Mohammadsaleh, *Catal. Lett.* **2018**, *148*, 1035.
- [48] M. Esmaeilpour, S. Zahmatkesh, N. Fahimi, M. Nosratabadi, *Appl. Organomet. Chem.* **2018**, *32*, e4302.
- [49] A. R. Hajipour, P. Abolfathi, F. Mohammadsaleh, *RSC Adv.* **2016**, *6*, 78080.
- [50] H. Khojasteh, V. Mirkhani, M. Moghadam, S. Tangestaninejad, I. Mohammadpoor-Baltork, *J. Nanostruct.* **2015**, *5*, 271.
- [51] J.-H. Kim, J.-W. Kim, M. Shokouhimehr, Y.-S. Lee, *J. Org. Chem.* **2005**, *70*, 6714.
- [52] Y. Liu, X. Bai, S. Li, *Microporous and Mesoporous Mater.* **2018**, *260*, 40.
- [53] J. Wang, B. Xu, H. Sun, G. Song, *Tetrahedron Lett.* **2013**, *54*, 238.
- [54] P. Li, L. Wang, L. Zhang, G. W. Wang, *Adv. Synth. Catal.* **2012**, *354*, 1307.
- [55] B. Altava, M. I. Burguete, E. García-Verdugo, N. Karbass, S. V. Luis, A. Puzary, V. Sans, *Tetrahedron Lett.* **2006**, *47*, 2311.
- [56] A. Z. Wilczewska, I. Misztalewska, *Organometallics* **2014**, *33*, 5203.
- [57] M. Tukhani, F. Panahi, A. Khalafi-Nezhad, *ACS Sustainable Chem. Eng.* **2017**, *6*, 1456.
- [58] A. R. Hajipour, A. R. Sadeghi, Z. Khorsandi, *Appl. Organomet. Chem.* **2018**, *32*, e4112.
- [59] G. Hamasaka, S. Ichii, Y. Uozumi, *Adv. Synth. Catal.* **2018**, *360*, 1833.
- [60] S. Sharma, B. R. Sarkar, *Synth. Commun.* **2018**, *48*, 906.

How to cite this article: Kempasiddhaiah M, Kandathil V, Dateer RB, Sasidhar BS, Patil SA, Patil SA. Magnetite tethered mesoionic carbene-palladium (II): An efficient and reusable nanomagnetic catalyst for Suzuki-Miyaura and Mizoroki-Heck cross-coupling reactions in aqueous medium. *Appl Organometal Chem.* 2019;e4846. <https://doi.org/10.1002/aoc.4846>